Exact Vibration Analysis of Beams with Arbitrary Intermediate Elastic Supports, Concentrated Masses and Non-Classical Boundary Conditions Under an Axial Force Using Shape Function Method

Xingzhuang ZHAO
A. James Clark School of Engineering, University of Maryland, College Park, MD, 20740, USA. E-mail: xzzhao@umd.edu

Abstract: - Vibration analysis of beams with multiple intermediate elastic supports and concentrated masses under an axial force is of theoretical and practical importance. In this work, the mathematical model governing the vibrations of beams is reformulated and is solved by the shape function method. The exact and explicit vibration solutions for the non-conventional and conventional boundary conditions are derived, which are determined by four shape functions and four unknown constants. Parametric studies are performed to show that the conventional boundary conditions can be represented by the non-conventional elastic boundary conditions. Besides, the vibrations of multi-span continuous beams can also be simulated with the proposed method by increasing the stiffnesses of the intermediate elastic supports. The results reported in this work are potentially useful in structural health monitoring and damage detection.

Keywords: - SFM, frequency, Laplace transform, Euler-Bernoulli beam

1. INTRODUCTION

A beam with multiple intermediate elastic supports, concentrated masses, non-conventional boundary conditions under an axial force is of wide practical interest in civil engineering and mechanical engineering. The vibration responses of the above-mentioned beam are related to many factors, in particular, the intermediate supports [1-3], the magnitude of the attached masses [4], the axial load, and the boundary conditions. Investigations combinations of these factors on the vibrations of an Euler-Bernoulli beam have been presented in the references [5-12].

The theoretical approaches in the literature can be roughly categorized into three categories, i.e., Rayleigh-Ritz method, transfer matrix method, and Green's function method. The free vibration analysis of a continuous beam with multi-masses under an axial force was investigated by Laura et al. [13] and an approximate solution was achieved with the help of the classical Rayleigh-Ritz method. Bapat and Bapat [5] adopted the transfer matrix method to investigate the natural frequencies of a straight beam with multiple collocated translational and torsional supports, as well as lumped masses. To obtain the exact solution, the continuities of the displacement and slope, and the relationship between the shear force and moment at the intermediate support was implemented. Based on the work of Bapat and Bapat, Lin and Bapat [14] further studied the free and forced vibrations of a multi-supported beam.

Some of the representative investigations with the Green's function method can be found in reference [7-9, 15-19]. Green's function method was adopted by Kukla [7, 8, 16, 20] to carry out a series of vibration analysis of Euler-Bernoulli beams. Kukla [7] applied the Green's function method to study the vibration frequencies of beams with arbitrarily located intermediate elastic supports. In a follow-up study [20], Kukla investigated the frequency responses of a beam with collocated intermediate elastic supports and concentrated masses under a constant axial force. The beam was first discretized into $N + 1$ segments by the N intermediate supports or masses. Then the frequency equation was expressed by a determinant of order N. However, there are two major limitations of Kukla's investigation. First, the non-conventional elastic boundary conditions were not handled. Second, the order of the determinant is the same as the number of intermediate supports or masses, which is inefficient when the number of elastic supports is large.

In a recent investigation, based on the contribution of Kukla [7], Rončević et al. [9] studied the vibrations of Euler-Bernoulli beams with multiple intermediate elastic supports with non-conventional boundary conditions. Applying the Green's function method, the natural frequencies and mode shapes were obtained for 49 different sets of boundary conditions, which were yielded by combining seven boundary conditions: pinned, clamped, sliding, free, translational spring, rotational spring, and combined translational-rotational spring. However, the concentrated masses and the axial force were not incorporated in their model. The Shape Function Method (SFM) was introduced by the author to investigate the free vibration of a beam with multiple

elastic supports in a previous paper [21]. However, in the work, only the elastic supports were considered.

The research on vibration analysis of a beam with elastic supports, lumped masses, non-conventional boundary conditions under axial force is meaningful in many applications. For instance, the frequencies and mode shapes obtained by the vibration analysis is essential in structural health monitoring [22-29], damage detection [11, 30-35], vehicle-bridge interaction study [36-39].

The purpose of this study is to overcome the above-mentioned limitations of the Green's function method [7, 9] and extend the SFM [21, 40] to include the concentrated masses and axial force. The shape function method is adopted to obtain the frequency and mode shape equations of the free vibrations of Euler-Bernoulli beams with an arbitrary number of intermediate elastic supports, concentrated masses, and non-conventional boundary conditions under an axial force.

2. Equation of motion

The typical Euler-Bernoulli beam with arbitrary elastic supports and concentrated masses under axial force is shown in Figure 1, and it is assumed that boundary conditions of the beam are simulated by translational-rotational elastic supports.

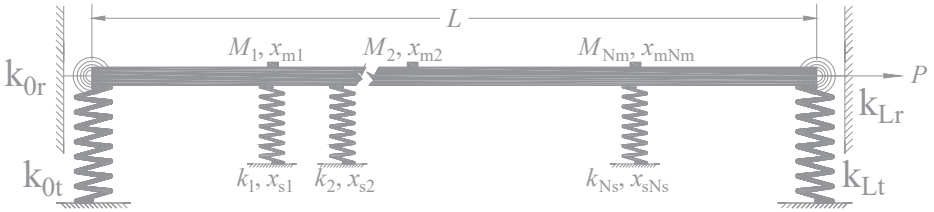

Figure 1. A beam with arbitrary intermediate elastic supports, concentrated masses, and an axial force under non-conventional boundary conditions

The beam segment with arbitrary intermediate supports, concentrated masses, and an axial force undergoing transverse vibration is shown in Figure 2(a). The forces acting on an infinitesimal element of length dx are presented in Figure 2(b).

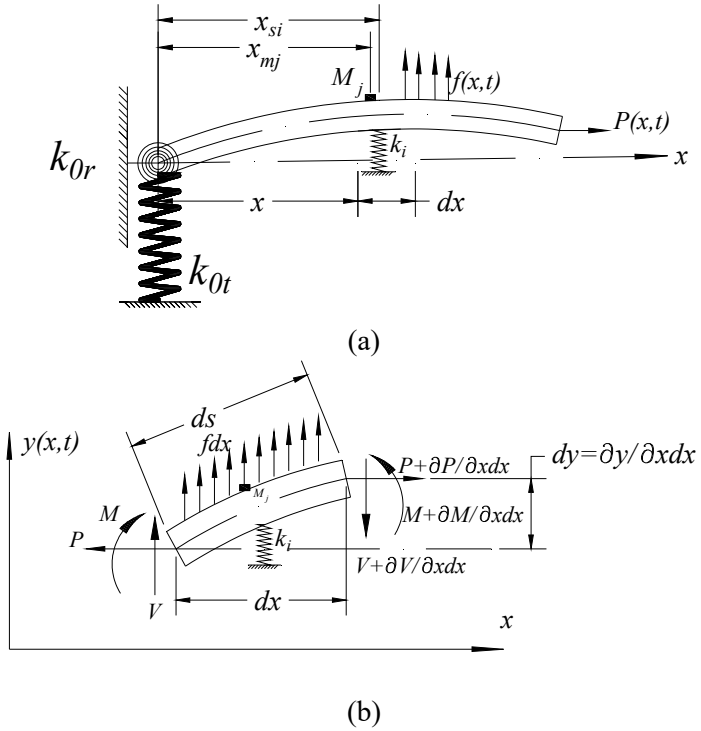

Figure 2. A beam with arbitrary translational elastic supports and concentrated masses under axial force. (a) A segment of a beam with elastic boundary conditions. (b) Forces on an infinitesimal element

When the amplitudes of vibration are small, the variation of the length of the beam element in Figure 2 (b) is approximated as

$$\boldsymbol{ds - dx = \sqrt{dx^2 + dy^2} - dx \approx \frac{1}{2}\left(\frac{\partial y(x,t)}{\partial x}\right)^2 dx} \quad (1)$$

Assuming the small displacement of the vibration does not result in changes in the axial force $P(x,t)$

and the transverse distributed force $f(x,t)$ [41], the work due to the axial force against the variation of the length of the beam element can be written as

$$W_p = -\frac{1}{2}\int_0^L P\left(\frac{\partial y(x,t)}{\partial x}\right)^2 dx \quad (2)$$

The work done by the transverse load and the intermediate translational elastic support is

$$W_t = \int_0^L \left[f(x,t)y(x,t) - \frac{1}{2}\sum_{i=1}^{N_s} k_i\,\delta(x - x_{si})y^2(x,t)\right] dx \quad (3)$$

Therefore, the total work due to the axial force, the transverse load, and the translational elastic support is given by

$$W = W_p + W_t \quad (4)$$

In Eq. (3), Dirac's delta function $\delta(x)$D is introduced, which is different from the conventional functions and has unique properties [21].

Besides, the strain energy of the beam is expressed as

$$\Pi = \frac{1}{2}\int_0^L E(x)I(x)\left(\frac{\partial^2 y(x,t)}{\partial x^2}\right)^2 dx \quad (5)$$

and the kinetic energy is written as

$$\mathrm{T} = \int_0^L \left[\frac{1}{2}\rho(x)A(x)\left(\frac{\partial y(x,t)}{\partial t}\right)^2 + \frac{1}{2}\sum_{j=1}^{N_m} M_j\,\delta(x - x_{mj})\left(\frac{\partial y(x,t)}{\partial t}\right)^2\right] dx \quad (6)$$

According to the extended Hamilton's principle,

$$\delta\int_{t_1}^{t_2}(T - \Pi + \mathrm{W})dt = 0 \quad (7)$$

Note that, fully aware of the abuse of the notation δ, this symbol is also used to represent the Dirac's delta function as in $M_j\,\delta(x - x_{mj})$ and $k_i\delta(x - x_{si})$, which should be clear to the reader.

Each of the three terms in Eq. (7) can be evaluated separately as follows. For the term with kinetic energy,

$$\delta\int_{t_1}^{t_2} T\,dt = \int_0^L\int_{t_1}^{t_2}\left[\rho(x)A(x) + \sum_{j=1}^{N_m} M_j\,\delta(x - x_{mj})\right]\frac{\partial y(x,t)}{\partial t}\frac{\partial}{\partial t}(\delta\mathrm{y}(\mathrm{x},\mathrm{t}))dt\,dx \quad (8)$$

Assuming $\delta y(x,t_1) = \delta y(x,t_2) = 0$, integration by parts of Eq. (8) yields

$$\delta\int_{t_1}^{t_2} T\,dt = -\int_{t_1}^{t_2}\int_0^L\left[\rho(x)A(x) + \sum_{j=1}^{N_m} M_j\,\delta(x - x_{mj})\right]\frac{\partial^2 y(x,t)}{\partial t^2}\delta\mathrm{y}(\mathrm{x},\mathrm{t})dxdt \quad (9)$$

Similarly, for the term with strain energy,

$$\delta\int_{t_1}^{t_2}\Pi\,dt = \int_{t_1}^{t_2}\int_0^L E(x)I(x)\frac{\partial^2 y(x,t)}{\partial x^2}\delta\left(\frac{\partial^2 y(x,t)}{\partial x^2}\right)dxdt \quad (10)$$

Integration by parts twice results in

$$\delta\int_{t_1}^{t_2}\Pi\,dt = \int_{t_1}^{t_2}\left[E(x)I(x)\frac{\partial^2 y(x,t)}{\partial x^2}\frac{\partial}{\partial x}(\delta\mathrm{y}(\mathrm{x},\mathrm{t}))\right|_0^L - \frac{\partial}{\partial x}\left(E(x)I(x)\frac{\partial^2 y(x,t)}{\partial x^2}\right)\delta\mathrm{y}(\mathrm{x},\mathrm{t})\Big|_0^L + \int_0^L\frac{\partial^2}{\partial x^2}\left(E(x)I(x)\frac{\partial^2 y(x,t)}{\partial x^2}\right)\delta\mathrm{y}(\mathrm{x},\mathrm{t})\,dx\Big]dt \quad (11)$$

The variation of the work is evaluated as

$$\delta\int_{t_1}^{t_2}\mathrm{W}\,dt = \int_{t_1}^{t_2}\int_0^L\left[-P\frac{\partial y(x,t)}{\partial x} + f(x,t) - \sum_{i=1}^{N_s} k_i\,\delta(x - x_{si})y(x,t)\right]\delta\mathrm{y}(\mathrm{x},\mathrm{t})dxdt \quad (12)$$

Integration by parts of the first term in the right-hand side yields

$$\delta\int_{t_1}^{t_2}\mathrm{W}\,dt = -\int_{t_1}^{t_2} P\frac{\partial y(x,t)}{\partial x}\delta\mathrm{y}(\mathrm{x},\mathrm{t})\Big|_0^L dt + \int_{t_1}^{t_2}\int_0^L\left[P\frac{\partial^2 y(x,t)}{\partial x^2} + f(x,t) - \sum_{i=1}^{N_s} k_i\,\delta(x - x_{si})y(x,t)\right]\delta y(x,t)\,dx\,dt \quad (13)$$

Substituting the obtained results in Eqs. (9), (11), and (13) into Eq. (7) gives

$$\int_{t_1}^{t_2}\int_0^L\left\{-\left[\rho(x)A(x) + \sum_{j=1}^{N_m} M_j\,\delta(x - x_{mj})\right]\frac{\partial^2 y(x,t)}{\partial t^2} - \frac{\partial^2}{\partial x^2}\left(E(x)I(x)\frac{\partial^2 y(x,t)}{\partial x^2}\right) + P\frac{\partial^2 y(x,t)}{\partial x^2} + f(x,t) - \sum_{i=1}^{N_s} k_i\,\delta(x - x_{si})y(x,t)\right\}\delta y(x,t)dx\,dt - \int_{t_1}^{t_2}\left[P\frac{\partial y(x,t)}{\partial x} - \frac{\partial}{\partial x}\left(E(x)I(x)\frac{\partial^2 y(x,t)}{\partial x^2}\right)\right]\delta\mathrm{y}(\mathrm{x},\mathrm{t})\Big|_0^L dt - \int_{t_1}^{t_2} E(x)I(x)\frac{\partial^2 y(x,t)}{\partial x^2}\frac{\partial}{\partial x}(\delta\mathrm{y}(\mathrm{x},\mathrm{t}))\Big|_0^L dt = 0 \quad (14)$$

As the variation $\delta y(x,t)$ in Eq. (14) is arbitrary, the general differential equation governing the free transverse vibration of a beam is obtained as

$$\frac{\partial^2}{\partial x^2}\left[E(x)I(x)\frac{\partial^2 y(x,t)}{\partial x^2}\right] + \rho(x)A(x)\frac{\partial^2 y(x,t)}{\partial t^2} + \sum_{j=1}^{N_m} M_j\,\delta(x - x_{mj})\frac{\partial^2 y(x,t)}{\partial t^2} + \sum_{i=1}^{N_s} k_i\,\delta(x - x_{si})y(x,t) - P\frac{\partial^2 y(x,t)}{\partial x^2} = 0 \quad (15)$$

in which $y(x,t)$ denotes the displacement, $I(x)$ and $A(x)$ denote the moment of inertia and area, respectively, and $E(x)$ and $\rho(x)$ denote Young's modulus and density, respectively, x_{si} denotes the position of the i^{th} elastic support, k_i denotes the translational stiffness of the i^{th} elastic support and N_s denotes the total number of supports, x_{mj} is the position of the i^{th} mass, M_j denotes the mass at position x_{mj}, P denotes the axial force and is assumed to be constant. In the present work, $E(x)I(x) = E_0I_0$ and $\rho(x)A(x) = \rho_0A_0$ are assumed.

Assuming the following expression is valid,

$$y(x,t) = Y(x)W(t) \quad (16)$$

Insert Eq. (16) into Eq. (15), performing the technique of separation of variables yields

$$E_0I_0Y^{(iv)}(x) - \omega^2\rho_0A_0Y(x) - \omega^2\sum_{j=1}^{N_m} M_j\,\delta(x - x_{mj})Y(x) + \sum_{i=1}^{N_s} k_i\,\delta(x - x_{si})Y(x) - PY''(x) = 0 \quad (17)$$

By introducing the non-dimensional coordinate $\xi = \frac{x}{L}$ and noticing that $0 \le \xi \le 1$ [42], the following non-dimensional position parameters are defined

$$\xi_{mj} = \frac{x_{mj}}{L} \quad (18)$$

$$\xi_{si} = \frac{x_{si}}{L} \quad (19)$$

$$\phi(\xi) = \frac{Y(\xi)}{L} \quad (20)$$

Using the above non-dimensional variables, Eq. (17) can be rewritten as

$$\phi^{(iv)}(\xi) - \beta^4\phi(\xi) - \beta^4\sum_{j=1}^{N_m}\eta_{mj}\,\delta(\xi - \xi_{mj})\phi(\xi) + \sum_{i=1}^{N_s} K_i\,\delta(\xi - \xi_{si})\phi(\xi) - 2\Gamma\phi''(\xi) = 0 \quad (21)$$

in which $\beta = \sqrt[4]{\frac{\omega^2 \rho_0 A_0 L^4}{E_0 I_0}}$, $\eta_{mj} = \frac{M_j}{\rho_0 A_0 L}$ represents the non-dimensional mass parameter, $\Gamma = \frac{TL^2}{2E_0 I_0}$ denotes the non-dimensional axial force, and $K_i = \frac{k_i L^3}{E_0 I_0}$ denotes the non-dimensional stiffness of the i^{th} support.

3. EXACT AND EXPLICIT MODE SHAPE SOLUTION

Carrying out Laplace transform on Eq. (21) gives,

$$\boldsymbol{s^4\Phi(s) - s^3\phi(0) - s^2\phi'(0) - s\phi''(0) - \phi'''(0) - \beta^4\Phi(s) - \beta^4\sum_{j=1}^{N_m}\eta_{mj}\,\phi(\xi_{mj})e^{-s\xi_{mj}} + \sum_{i=1}^{N_s}K_i\,\phi(\xi_{si})e^{-s\xi_{si}} - 2\Gamma[s^2\Phi(s) - s\phi(0) - \phi'(0)] = 0} \quad (22)$$

where $\Phi(s) = \mathcal{L}\{\phi(\xi)\}$, and $\phi^i(0)\ i = 0,1,2,$ and 3 are the derivatives of $\phi(\xi)$ at $\xi = 0$.

To simplify the calculation, the following two variables are introduced,

$$\boldsymbol{\alpha = \sqrt{\sqrt{\Gamma^2 + \beta^4} + \Gamma}} \quad (23)$$

$$\boldsymbol{\gamma = \sqrt{\sqrt{\Gamma^2 + \beta^4} - \Gamma}} \quad (24)$$

Introducing the following definitions for the inverse Laplace of the terms in Eq. (22) as follows

$$\boldsymbol{\mathcal{L}^{-1}\left\{\frac{s^3}{s^4-2\Gamma s^2-\beta^4}\right\} = \frac{\alpha^2\cosh(\alpha\xi)+\gamma^2\cos(\gamma\xi)}{\alpha^2+\gamma^2} \triangleq S_0(\xi)} \quad (25)$$

$$\boldsymbol{\mathcal{L}^{-1}\left\{\frac{s^2}{s^4-2\Gamma s^2-\beta^4}\right\} = \frac{\alpha\sinh(\alpha\xi)+\gamma\sin(\gamma\xi)}{\alpha^2+\gamma^2} \triangleq S_1(\xi)} \quad (26)$$

$$\boldsymbol{\mathcal{L}^{-1}\left\{\frac{s}{s^4-2\Gamma s^2-\beta^4}\right\} = \frac{\cosh(\alpha\xi)-\cos(\gamma\xi)}{\alpha^2+\gamma^2} \triangleq S_2(\xi)} \quad (27)$$

$$\boldsymbol{\mathcal{L}^{-1}\left\{\frac{1}{s^4-2\Gamma s^2-\beta^4}\right\} = \frac{\gamma\sinh(\alpha\xi)-\alpha\sin(\gamma\xi)}{\alpha\gamma(\alpha^2+\gamma^2)} \triangleq S_3(\xi)} \quad (28)$$

Applying the inverse Laplace transform and adopting the foregoing defined functions yields the solution of Eq. (21) as

$$\boldsymbol{\phi(\xi) = \phi(0)[S_0(\xi) - 2\Gamma S_2(\xi)] + \phi'(0)[S_1(\xi) - 2\Gamma S_3(\xi)] + \phi''(0)S_2(\xi) + \phi'''(0)S_3(\xi) + \beta^4\sum_{j=1}^{N_m}\eta_j\,S_3(\xi-\xi_{mj})\phi(\xi_{mj})H(\xi-\xi_{mj}) - \sum_{j=1}^{N_s}K_{sj}\,S_3(\xi-\xi_{sj})\phi(\xi_{sj})H(\xi-\xi_{sj})} \quad (29)$$

Substituting $\xi = \xi_{si}\ (i = 1,2,\dots,N_s)$ into Eq. (29) yields a system of N_s equations,

$$\boldsymbol{\phi(\xi_{si}) + \sum_{j=1}^{N_s}K_j\,S_3(\xi_{si}-\xi_{sj})\phi(\xi_{sj})H(\xi_{si}-\xi_{sj}) - \beta^4\sum_{k=1}^{N_m}\eta_{mk}\,S_3(\xi_{si}-\xi_{mk})\phi(\xi_{mk})H(\xi_{si}-\xi_{mk}) = \phi(0)[S_0(\xi_{si}) - 2\Gamma S_2(\xi_{si})] + \phi'(0)[S_1(\xi_{si}) - 2\Gamma S_3(\xi_{si})] + \phi''(0)S_2(\xi_{si}) + \phi'''(0)S_3(\xi_{si})} \quad (30)$$

Similarly, substituting $\xi = \xi_{mi}\ (i = 1,2,\dots,N_m)$ into Eq. (29) yields a system of N_m equations,

$$\boldsymbol{\phi(\xi_{mi}) + \sum_{j=1}^{N_s}K_j\,S_3(\xi_{mi}-\xi_{sj})\phi(\xi_{sj})H(\xi_{mi}-\xi_{sj}) - \beta^4\sum_{k=1}^{N_m}\eta_{mk}\,S_3(\xi_{mi}-\xi_{mk})\phi(\xi_{mk})H(\xi_{mi}-\xi_{mk}) = \phi(0)[S_0(\xi_{mi}) - 2\Gamma S_2(\xi_{mi})] + \phi'(0)[S_1(\xi_{mi}) - 2\Gamma S_3(\xi_{mi})] + \phi''(0)S_2(\xi_{mi}) + \phi'''(0)S_3(\xi_{mi})} \quad (31)$$

Eqs. (30) and (31) give a total of $N_s + N_m$ equations, which is equal to the number of unknowns, i.e., $\phi(\xi_{sj})$ and $\phi(\xi_{mj})$. Thus, the explicit solution of Eq. (21) can be achieved. However, in engineering applications, some of the concentrated masses may be collocated with the translational elastic supports, i.e., $\xi_{sj} = \xi_{mk}$, leading to $\phi(\xi_{sj}) = \phi(\xi_{mk})$, which would reduce the number of unknowns. In order to minimize the number of unknowns, one needs to renumber the intermediate supports and concentrated masses, as well as the corresponding positions of them.

Assuming there are N_{sm} concentrated masses and elastic supports that are located at the same positions, Then the number of concentrated masses that are not collocated with elastic supports are $N_m - N_{sm}$ and the number of elastic supports that are not collocated with concentrated masses are $N_s - N_{sm}$. The author labels the elastic supports and concentrated masses, together with the positions of the supports and masses, according to the following rules.

First, label the collocated concentrated mass and elastic supports with the same number. Second, label the elastic supports that are not collocated with the concentrated masses. Lastly, label the non-collocated concentrated masses.

For a beam with three elastic supports and three concentrated masses with one collocated mass and elastic support as shown in Figure 3, i.e., $N_s = 3$, $N_m = 3$, N_{sm}=1, the labels of the elastic supports and concentrated masses as well as the corresponding positions are presented according to the above rules. In Figure 3, the elastic support K_j and mass η_1 share the same position ξ_1.

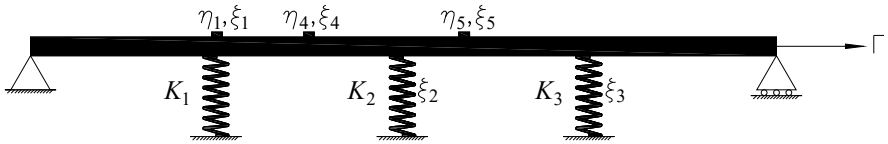

Figure 3. The labels of the elastic supports and concentrated masses

Based on the above rules, Eqs. (30) and (31) can be incorporated into one form as shown in the following equation (Eq. (32)),

$$\boldsymbol{\phi}(\xi_i) + \sum_{j=1}^{N_{sm}}[\boldsymbol{K_j} - \boldsymbol{\beta^4\eta_j}]\boldsymbol{S_3}(\xi_i - \xi_j)\boldsymbol{\phi}(\xi_j)\boldsymbol{H}(\xi_i - \xi_j) + \sum_{k=N_{sm}+1}^{N_s}\boldsymbol{K_k}\,\boldsymbol{S_3}(\xi_i - \xi_k)\boldsymbol{\phi}(\xi_k)\boldsymbol{H}(\xi_i - \xi_k) - \boldsymbol{\beta^4}\sum_{l=N_s+1}^{N_m+N_s-N_{sm}}\boldsymbol{\eta_l}\,\boldsymbol{S_3}(\xi_i - \xi_l)\boldsymbol{\phi}(\xi_l)\boldsymbol{H}(\xi_i - \xi_l) = \boldsymbol{\phi}(\mathbf{0})[\boldsymbol{S_0}(\xi_i) - \mathbf{2\Gamma}\boldsymbol{S_2}(\xi_i)] + \boldsymbol{\phi}'(\mathbf{0})[\boldsymbol{S_1}(\xi_i) - \mathbf{2\Gamma}\boldsymbol{S_3}(\xi_i)] + \boldsymbol{\phi}''(\mathbf{0})\boldsymbol{S_2}(\xi_i) + \boldsymbol{\phi}'''(\mathbf{0})\boldsymbol{S_3}(\xi_i) \quad (32)$$

In Eq. (32), the second term on the left-hand sides denotes the contribution of the collocated elastic supports and concentrated masses, the third term represents the influences of the non-collocated intermediate supports, and the fourth term denotes the contribution of the non-collocated concentrated masses.

Or concisely in matrix form,

$$\boldsymbol{\Omega\phi} = \boldsymbol{\varphi} \quad (33)$$

where Ω denotes a matrix of the size $(N_s + N_m - N_{sm}) \times (N_s + N_m - N_{sm})$, $\phi = [\phi(\xi_1), \phi(\xi_2), \ldots, \phi(\xi_{N_s+N_m-N_{sm}})]^T$ is a column vector of size $(N_s + N_m - N_{sm}) \times 1$ and $\varphi = [\varphi(\xi_1), \varphi(\xi_2), \ldots, \varphi(\xi_{N_s+N_m-N_{sm}})]^T$ is a column vector of size $(N_s + N_m - N_{sm}) \times 1$, and the superscript T indicates transpose of the vector.

In Eq. (33), the unknown deflections at the elastic supports and concentrated masses can be rewritten as

$$\boldsymbol{\phi_i} = \boldsymbol{\phi}(\boldsymbol{\xi_i}) \quad (34)$$

and the column vector on the right-hand side of Eq. (33) is defined as

$$\boldsymbol{\varphi_j} = \boldsymbol{\phi}(\mathbf{0})\big[\boldsymbol{S_0}(\boldsymbol{\xi_j}) - \mathbf{2\Gamma}\boldsymbol{S_2}(\boldsymbol{\xi_j})\big] + \boldsymbol{\phi}'(\mathbf{0})\big[\boldsymbol{S_1}(\boldsymbol{\xi_j}) - \mathbf{2\Gamma}\boldsymbol{S_3}(\boldsymbol{\xi_j})\big] + \boldsymbol{\phi}''(\mathbf{0})\boldsymbol{S_2}(\boldsymbol{\xi_j}) + \boldsymbol{\phi}'''(\mathbf{0})\boldsymbol{S_3}(\boldsymbol{\xi_j}) \quad (35)$$

Besides, in element form, Ω can be written in Eq. (36),

$$\boldsymbol{\Omega_{ij}} = \begin{cases} \mathbf{1} & \boldsymbol{if\ i = j} \\ [\boldsymbol{K_j} - \boldsymbol{\beta^4\eta_j}]\boldsymbol{S_3}(\xi_i - \xi_j)\boldsymbol{H}(\xi_i - \xi_j) & \boldsymbol{if\ i \neq j\ (1 \le j \le N_{sm})} \\ \boldsymbol{K_j}\boldsymbol{S_3}(\xi_i - \xi_j)\boldsymbol{H}(\xi_i - \xi_j) & \boldsymbol{if\ i \neq j\ (N_{sm} + 1 \le j \le N_s)} \\ -\boldsymbol{\beta^4\eta_j}\boldsymbol{S_3}(\xi_i - \xi_j)\boldsymbol{H}(\xi_i - \xi_j) & \boldsymbol{if\ i \neq j\ (N_s + 1 \le j \le N_m + N_s - N_{sm})} \end{cases} \quad (36)$$

The displacements of the elastic support and/or concentrated masses can be obtained as $\phi = \Omega^{-1}\varphi$. In element form, and adopting the Einstein convention, the unknown deflections at the elastic supports and the concentrated masses are solved as $\phi_i = \Omega_{ij}^{-1}\varphi_j$. Introducing $\phi_i$into Eq. (29), the explicit mode shape can be written in Eq. (37)

$$\boldsymbol{\phi}(\xi) = \boldsymbol{\phi}(\mathbf{0})[\boldsymbol{S_0}(\xi) - \mathbf{2\Gamma}\boldsymbol{S_2}(\xi)] + \boldsymbol{\phi}'(\mathbf{0})[\boldsymbol{S_1}(\xi) - \mathbf{2\Gamma}\boldsymbol{S_3}(\xi)] + \boldsymbol{\phi}''(\mathbf{0})\boldsymbol{S_2}(\xi) + \boldsymbol{\phi}'''(\mathbf{0})\boldsymbol{S_3}(\xi) - \sum_{i=1}^{N_{sm}}[\boldsymbol{K_i} - \boldsymbol{\beta^4\eta_i}]\boldsymbol{S_3}(\xi - \xi_i)\boldsymbol{\Omega_{ij}^{-1}}\boldsymbol{\varphi_j}\boldsymbol{H}(\xi - \xi_i) - \sum_{i=N_{sm}+1}^{N_s}\boldsymbol{K_i}\,\boldsymbol{S_3}(\xi - \xi_i)\boldsymbol{\Omega_{ij}^{-1}}\boldsymbol{\varphi_j}\boldsymbol{H}(\xi - \xi_i) + \boldsymbol{\beta^4}\sum_{i=N_s+1}^{N_m+N_s-N_{sm}}\boldsymbol{\eta_i}\,\boldsymbol{S_3}(\xi - \xi_i)\boldsymbol{\Omega_{ij}^{-1}}\boldsymbol{\varphi_j}\boldsymbol{H}(\xi - \xi_i) \quad (37)$$

Performing some simple algebra manipulations gives the exact and explicit solution in Eq. (38),

$$\boldsymbol{\phi}(\xi) = \boldsymbol{\phi}(\mathbf{0})[\boldsymbol{S_0}(\xi) - \mathbf{2\Gamma}\boldsymbol{S_2}(\xi) - \sum_{i=1}^{N_{sm}}[\boldsymbol{K_i} - \boldsymbol{\beta^4\eta_i}]\boldsymbol{S_3}(\xi - \xi_i)\boldsymbol{\Omega_{ij}^{-1}}\left(\boldsymbol{S_0}(\xi_j) - \mathbf{2\Gamma}\boldsymbol{S_2}(\xi_j)\right)\boldsymbol{H}(\xi - \xi_i) - \sum_{i=N_{sm}+1}^{N_s}\boldsymbol{K_i}\,\boldsymbol{S_3}(\xi - \xi_i)\boldsymbol{\Omega_{ij}^{-1}}(\boldsymbol{S_0}(\xi_j) - \mathbf{2\Gamma}\boldsymbol{S_2}(\xi_j))\boldsymbol{H}(\xi - \xi_i) + \boldsymbol{\beta^4}\sum_{i=N_s+1}^{N_m+N_s-N_{sm}}\boldsymbol{\eta_i}\,\boldsymbol{S_3}(\xi - \xi_i)\boldsymbol{\Omega_{ij}^{-1}}(\boldsymbol{S_0}(\xi_j) - \mathbf{2\Gamma}\boldsymbol{S_2}(\xi_j))\boldsymbol{H}(\xi - \xi_i)] + \boldsymbol{\phi}'(\mathbf{0})[\boldsymbol{S_1}(\xi) - \mathbf{2\Gamma}\boldsymbol{S_3}(\xi) - \sum_{i=1}^{N_{sm}}[\boldsymbol{K_i} - \boldsymbol{\beta^4\eta_i}]\boldsymbol{S_3}(\xi - \xi_j)\boldsymbol{\Omega_{ij}^{-1}}\left(\boldsymbol{S_1}(\xi_j) - \mathbf{2\Gamma}\boldsymbol{S_3}(\xi_j)\right)\boldsymbol{H}(\xi - \xi_j) - \sum_{i=N_{sm}+1}^{N_s}\boldsymbol{K_i}\,\boldsymbol{S_3}(\xi - \xi_i)\boldsymbol{\Omega_{ij}^{-1}}(\boldsymbol{S_1}(\xi_j) - \mathbf{2\Gamma}\boldsymbol{S_3}(\xi_j))\boldsymbol{H}(\xi - \xi_i) + \boldsymbol{\beta^4}\sum_{i=N_s+1}^{N_m+N_s-N_{sm}}\boldsymbol{\eta_i}\,\boldsymbol{S_3}(\xi - \xi_i)\boldsymbol{\Omega_{ij}^{-1}}(\boldsymbol{S_1}(\xi_j) - \mathbf{2\Gamma}\boldsymbol{S_3}(\xi_j))\boldsymbol{H}(\xi - \xi_i)] + \boldsymbol{\phi}''(\mathbf{0})[\boldsymbol{S_2}(\xi) - \sum_{j=1}^{N_{sm}}[\boldsymbol{K_i} - \boldsymbol{\beta^4\eta_i}]\boldsymbol{S_3}(\xi - \xi_i)\boldsymbol{\Omega_{ij}^{-1}}\boldsymbol{S_2}(\xi_j)\boldsymbol{H}(\xi - \xi_i) - \sum_{i=N_{sm}+1}^{N_s}\boldsymbol{K_i}\,\boldsymbol{S_3}(\xi - \xi_i)\boldsymbol{\Omega_{ij}^{-1}}\boldsymbol{S_2}(\xi_j)\boldsymbol{H}(\xi - \xi_i) + \boldsymbol{\beta^4}\sum_{i=N_s+1}^{N_m+N_s-N_{sm}}\boldsymbol{\eta_i}\,\boldsymbol{S_3}(\xi - \xi_i)\boldsymbol{\Omega_{ij}^{-1}}\boldsymbol{S_2}(\xi_j)\boldsymbol{H}(\xi - \xi_i)] + \boldsymbol{\phi}'''(\mathbf{0})[\boldsymbol{S_3}(\xi) - \sum_{i=1}^{N_{sm}}[\boldsymbol{K_i} - \boldsymbol{\beta^4\eta_i}]\boldsymbol{S_3}(\xi - \xi_i)\boldsymbol{\Omega_{ij}^{-1}}\boldsymbol{S_3}(\xi_j)\boldsymbol{H}(\xi - \xi_i) - \sum_{i=N_{sm}+1}^{N_s}\boldsymbol{K_i}\,\boldsymbol{S_3}(\xi - \xi_i)\boldsymbol{\Omega_{ij}^{-1}}\boldsymbol{S_3}(\xi_j)\boldsymbol{H}(\xi - \xi_i) + \boldsymbol{\beta^4}\sum_{i=N_s+1}^{N_m+N_s-N_{sm}}\boldsymbol{\eta_i}\,\boldsymbol{S_3}(\xi - \xi_i)\boldsymbol{\Omega_{ij}^{-1}}\boldsymbol{S_3}(\xi_j)\boldsymbol{H}(\xi - \xi_i)] \quad (38)$$

4. BOUNDARY CONDITIONS

According to [21], the general boundary conditions of a beam (see Figure 1) with translational and rotational elastic supports at the two ends can be written as

$$\boldsymbol{\phi}'''(\mathbf{0}) = -\boldsymbol{K_{0t}}\boldsymbol{\phi}(\mathbf{0}) \quad (39)$$

$$\boldsymbol{\phi}''(\mathbf{0}) = \boldsymbol{K_{0r}}\boldsymbol{\phi}'(\mathbf{0}) \quad (40)$$

$$\boldsymbol{\phi}'''(\mathbf{1}) = \boldsymbol{K_{1t}}\boldsymbol{\phi}(\mathbf{1}) \quad (41)$$

$$\boldsymbol{\phi}''(\mathbf{1}) = -\boldsymbol{K_{1r}}\boldsymbol{\phi}'(\mathbf{1}) \quad (42)$$

where $K_{0t} = \frac{k_{0t}L^3}{E_0 I_0}, K_{0r} = \frac{k_{0r}L}{E_0 I_0}, K_{1t} = \frac{k_{Lt}L^3}{E_0 I_0}$, and $K_{1r} = \frac{k_{Lr}L}{E_0 I_0}$.

5. Frequency equation and mode shape function

Assuming the mode shape can be simplified as

$$\boldsymbol{\phi}(\xi) = \boldsymbol{\phi}(\mathbf{0})\boldsymbol{\Psi_0}(\xi) + \boldsymbol{\phi}'(\mathbf{0})\boldsymbol{\Psi_1}(\xi) + \boldsymbol{\phi}''(\mathbf{0})\boldsymbol{\Psi_2}(\xi) + \boldsymbol{\phi}'''(\mathbf{0})\boldsymbol{\Psi_3}(\xi) \quad (43)$$

where $\Psi_j(\xi) = S_j(\xi)$ $(j = 0, 1, 2 \text{ and } 3)$ are defined as

$$\boldsymbol{\Psi_0}(\xi) = \boldsymbol{S_0}(\xi) - \mathbf{2\Gamma}\boldsymbol{S_2}(\xi) - \sum_{i=1}^{N_{sm}}[\boldsymbol{K_i} - \boldsymbol{\beta^4\eta_i}]\boldsymbol{S_3}(\xi - \xi_i)\boldsymbol{\Omega_{ij}^{-1}}\left(\boldsymbol{S_0}(\xi_j) - \mathbf{2\Gamma}\boldsymbol{S_2}(\xi_j)\right)\boldsymbol{H}(\xi - \xi_i) -$$

$$\sum_{i=N_{sm}+1}^{N_s} \boldsymbol{K_i}\, \boldsymbol{S_3}(\xi-\xi_i)\boldsymbol{\Omega_{ij}^{-1}}(\boldsymbol{S_0}(\xi_j)-\boldsymbol{2\Gamma S_2}(\xi_j))\boldsymbol{H}(\xi-\xi_i)+\boldsymbol{\beta^4}\sum_{i=N_s+1}^{N_m+N_s-N_{sm}}\boldsymbol{\eta_i}\, \boldsymbol{S_3}(\xi-\xi_i)\boldsymbol{\Omega_{ij}^{-1}}(\boldsymbol{S_0}(\xi_j)-\boldsymbol{2\Gamma S_2}(\xi_j))\boldsymbol{H}(\xi-\xi_i) \quad (44)$$

$$\boldsymbol{\Psi_1}(\xi)=\boldsymbol{S_1}(\xi)-\boldsymbol{2\Gamma S_3}(\xi)-\sum_{i=1}^{N_{sm}}[\boldsymbol{K_i}-\boldsymbol{\beta^4\eta_i}]\boldsymbol{S_3}(\xi-\xi_j)\boldsymbol{\Omega_{ij}^{-1}}\left(\boldsymbol{S_1}(\xi_j)-\boldsymbol{2\Gamma S_3}(\xi_j)\right)\boldsymbol{H}(\xi-\xi_j)-\sum_{i=N_{sm}+1}^{N_s}\boldsymbol{K_i}\,\boldsymbol{S_3}(\xi-\xi_i)\boldsymbol{\Omega_{ij}^{-1}}(\boldsymbol{S_1}(\xi_j)-\boldsymbol{2\Gamma S_3}(\xi_j))\boldsymbol{H}(\xi-\xi_i)+\boldsymbol{\beta^4}\sum_{i=N_s+1}^{N_m+N_s-N_{sm}}\boldsymbol{\eta_i}\,\boldsymbol{S_3}(\xi-\xi_i)\boldsymbol{\Omega_{ij}^{-1}}(\boldsymbol{S_1}(\xi_j)-\boldsymbol{2\Gamma S_3}(\xi_j))\boldsymbol{H}(\xi-\xi_i) \quad (45)$$

$$\boldsymbol{\Psi_2}(\xi)=\boldsymbol{S_2}(\xi)-\sum_{j=1}^{N_{sm}}[\boldsymbol{K_i}-\boldsymbol{\beta^4\eta_i}]\boldsymbol{S_3}(\xi-\xi_i)\boldsymbol{\Omega_{ij}^{-1}}\boldsymbol{S_2}(\xi_j)\boldsymbol{H}(\xi-\xi_i)-\sum_{i=N_{sm}+1}^{N_s}\boldsymbol{K_i}\,\boldsymbol{S_3}(\xi-\xi_i)\boldsymbol{\Omega_{ij}^{-1}}\boldsymbol{S_2}(\xi_j)\boldsymbol{H}(\xi-\xi_i)+\boldsymbol{\beta^4}\sum_{i=N_s+1}^{N_m+N_s-N_{sm}}\boldsymbol{\eta_i}\,\boldsymbol{S_3}(\xi-\xi_i)\boldsymbol{\Omega_{ij}^{-1}}\boldsymbol{S_2}(\xi_j)\boldsymbol{H}(\xi-\xi_i) \quad (46)$$

$$\boldsymbol{\Psi_3}(\xi)=\boldsymbol{S_3}(\xi)-\sum_{i=1}^{N_{sm}}[\boldsymbol{K_i}-\boldsymbol{\beta^4\eta_i}]\boldsymbol{S_3}(\xi-\xi_i)\boldsymbol{\Omega_{ij}^{-1}}\boldsymbol{S_3}(\xi_j)\boldsymbol{H}(\xi-\xi_i)-\sum_{i=N_{sm}+1}^{N_s}\boldsymbol{K_i}\,\boldsymbol{S_3}(\xi-\xi_i)\boldsymbol{\Omega_{ij}^{-1}}\boldsymbol{S_3}(\xi_j)\boldsymbol{H}(\xi-\xi_i)+\boldsymbol{\beta^4}\sum_{i=N_s+1}^{N_m+N_s-N_{sm}}\boldsymbol{\eta_i}\,\boldsymbol{S_3}(\xi-\xi_i)\boldsymbol{\Omega_{ij}^{-1}}\boldsymbol{S_3}(\xi_j)\boldsymbol{H}(\xi-\xi_i) \quad (47)$$

The above four functions are termed as the shape functions of a Euler-Bernoulli beam with multiple translational elastic supports and concentrated masses under an axial force. Combining Eq. (43) and Eqs. (39) – (42), yields Eq. (48), the form of which is the same as Ref. Applying the frequency equations [21],

$$\begin{bmatrix} \boldsymbol{\Psi_0'''(0)+K_{0t}} & \boldsymbol{\Psi_1'''(0)} & \boldsymbol{\Psi_2'''(0)} & \boldsymbol{\Psi_3'''(0)} \\ \boldsymbol{\Psi_0''(0)} & \boldsymbol{\Psi_1''(0)-K_{0r}} & \boldsymbol{\Psi_2''(0)} & \boldsymbol{\Psi_3''(0)} \\ \boldsymbol{\Psi_0'''(1)-\Psi_0(1)K_{1t}} & \boldsymbol{\Psi_1'''(1)-\Psi_1(1)K_{1t}} & \boldsymbol{\Psi_2'''(1)-\Psi_2(1)K_{1t}} & \boldsymbol{\Psi_3'''(1)-\Psi_3(1)K_{1t}} \\ \boldsymbol{\Psi_0''(1)+\Psi_0'(1)K_{1r}} & \boldsymbol{\Psi_1''(1)+\Psi_1'(1)K_{1r}} & \boldsymbol{\Psi_2''(1)+\Psi_2'(1)K_{1r}} & \boldsymbol{\Psi_3''(1)+\Psi_3'(1)K_{1r}} \end{bmatrix}\begin{pmatrix} \boldsymbol{\phi(0)} \\ \boldsymbol{\phi'(0)} \\ \boldsymbol{\phi''(0)} \\ \boldsymbol{\phi'''(0)} \end{pmatrix}=\begin{pmatrix} \boldsymbol{0} \\ \boldsymbol{0} \\ \boldsymbol{0} \\ \boldsymbol{0} \end{pmatrix} \quad (48)$$

The characteristic equation of the frequency is written as

$$\begin{vmatrix} \boldsymbol{\Psi_0'''(0)+K_{0t}} & \boldsymbol{\Psi_1'''(0)} & \boldsymbol{\Psi_2'''(0)} & \boldsymbol{\Psi_3'''(0)} \\ \boldsymbol{\Psi_0''(0)} & \boldsymbol{\Psi_1''(0)-K_{0r}} & \boldsymbol{\Psi_2''(0)} & \boldsymbol{\Psi_3''(0)} \\ \boldsymbol{\Psi_0'''(1)-\Psi_0(1)K_{1t}} & \boldsymbol{\Psi_1'''(1)-\Psi_1(1)K_{1t}} & \boldsymbol{\Psi_2'''(1)-\Psi_2(1)K_{1t}} & \boldsymbol{\Psi_3'''(1)-\Psi_3(1)K_{1t}} \\ \boldsymbol{\Psi_0''(1)+\Psi_0'(1)K_{1r}} & \boldsymbol{\Psi_1''(1)+\Psi_1'(1)K_{1r}} & \boldsymbol{\Psi_2''(1)+\Psi_2'(1)K_{1r}} & \boldsymbol{\Psi_3''(1)+\Psi_3'(1)K_{1r}} \end{vmatrix}=\boldsymbol{0} \quad (49)$$

According to [21], the frequency equation and mode shape function for the conventional boundary conditions can be written as.

(1): Pinned-Pinned

Characteristic equation (frequency)

$$\begin{vmatrix} \boldsymbol{\Psi_1(1)} & \boldsymbol{\Psi_3(1)} \\ \boldsymbol{\Psi_1''(1)} & \boldsymbol{\Psi_3''(1)} \end{vmatrix}=\boldsymbol{0} \quad (50)$$

Mode shape function

$$\boldsymbol{\phi}(\xi)=\boldsymbol{\phi'(0)\Psi_1}(\xi)+\boldsymbol{\phi'''(0)\Psi_3}(\xi) \quad (51)$$

(2) Clamped-Clamped

Characteristic equation (frequency)

$$\begin{vmatrix} \boldsymbol{\Psi_2(1)} & \boldsymbol{\Psi_3(1)} \\ \boldsymbol{\Psi_2'(1)} & \boldsymbol{\Psi_3'(1)} \end{vmatrix}=\boldsymbol{0} \quad (52)$$

Mode shape function

$$\boldsymbol{\phi}(\xi)=\boldsymbol{\phi''(0)\Psi_2}(\xi)+\boldsymbol{\phi'''(0)\Psi_3}(\xi) \quad (53)$$

(3): Clamped-Free

Characteristic equation (frequency)

$$\begin{vmatrix} \boldsymbol{\Psi_2''(1)} & \boldsymbol{\Psi_3''(1)} \\ \boldsymbol{\Psi_2'''(1)} & \boldsymbol{\Psi_3'''(1)} \end{vmatrix}=\boldsymbol{0} \quad (54)$$

Mode shape function

$$\boldsymbol{\phi}(\xi)=\boldsymbol{\phi''(0)\Psi_2}(\xi)+\boldsymbol{\phi'''(0)\Psi_3}(\xi) \quad (55)$$

(4): Clamped-Pinned

Characteristic equation (frequency)

$$\begin{vmatrix} \boldsymbol{\Psi_2(1)} & \boldsymbol{\Psi_3(1)} \\ \boldsymbol{\Psi_2''(1)} & \boldsymbol{\Psi_3''(1)} \end{vmatrix}=\boldsymbol{0} \quad (56)$$

Mode shape function

$$\boldsymbol{\phi}(\xi)=\boldsymbol{\phi''(0)\Psi_2}(\xi)+\boldsymbol{\phi'''(0)\Psi_3}(\xi) \quad (57)$$

It is worth noting that these frequency equations and mode shape functions share the same form as in [21], although the beams are different.

6. VERIFICATION

Two numerical examples are demonstrated in this section to show the validity of the developed theoretical model and the proposed shape function method (SFM). The first example comes from the published literature, which was solved by the Green's function method (GFM) by Kukla [20]. The obtained results by the current shape function method are compared with the original solutions by the Green's function method.

In the second example, a beam with 100 intermediate elastic supports and 100 concentrated masses under axial force is solved by implementing the shape function method. This example is purposely designed to illustrate that the proposed shape function can be applied to a large number of elastic supports and concentrated masses. Since it is known that when the numbers of elastic supports and masses are large and are evenly distributed along the beam, the vibration frequencies and mode shapes by the shape function method should be approaching to those of a beam on an elastic foundation with equivalent stiffness and mass.

6.1. Numerical example 1

As the first example, the symmetric beams with two intermediate translational elastic supports and two concentrated masses under axial force as shown in Figure 4. The numerical calculations are obtained for beams with different sets of boundary conditions, i.e., Pinned-Pinned (P-P) and Clamped-Clamped (C-C).

To examine the effects of the non-dimensional axial load Γ and concentrated masses $\eta_1 = \eta_2$ on the first four frequencies, the position parameter ξ_1 is continuously varied from 0 to 0.5. The stiffness of the supports $K_1 = K_2 = 1000$ are adopted. Besides, two cases of the axial force Γ are considered, i.e., $\Gamma = 50 \text{ or } 250$. The frequency response curves corresponding to three different cases of concentrated masses, i.e., $\eta_1 = \eta_2 = 0, 0.1, \text{or } 0.5$, are calculated. Applying Eqs. (50) and (52), the obtained frequency response curve of the first four modes for the P-P beam and C-C beam are shown in Figure 5 and Figure 6, respectively. To justify the validity of the proposed shape function method, the results obtained by the Green's function method in the literature [20] are also presented. As is observed from Figure 5 and Figure 6, the results by the shape function method comply very well with those of the Green's function method.

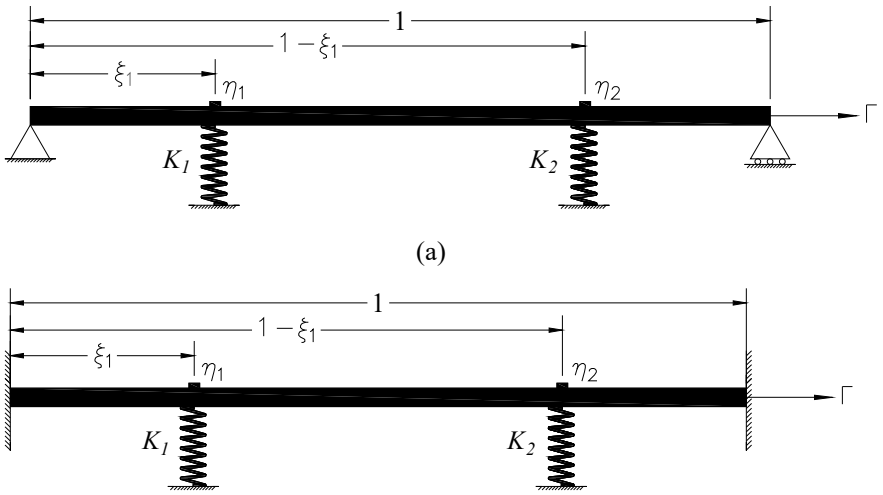

Figure 4. A beam with two intermediate translational elastic supports and two concentrated masses under axial force. (a) P-P. (b) C-C

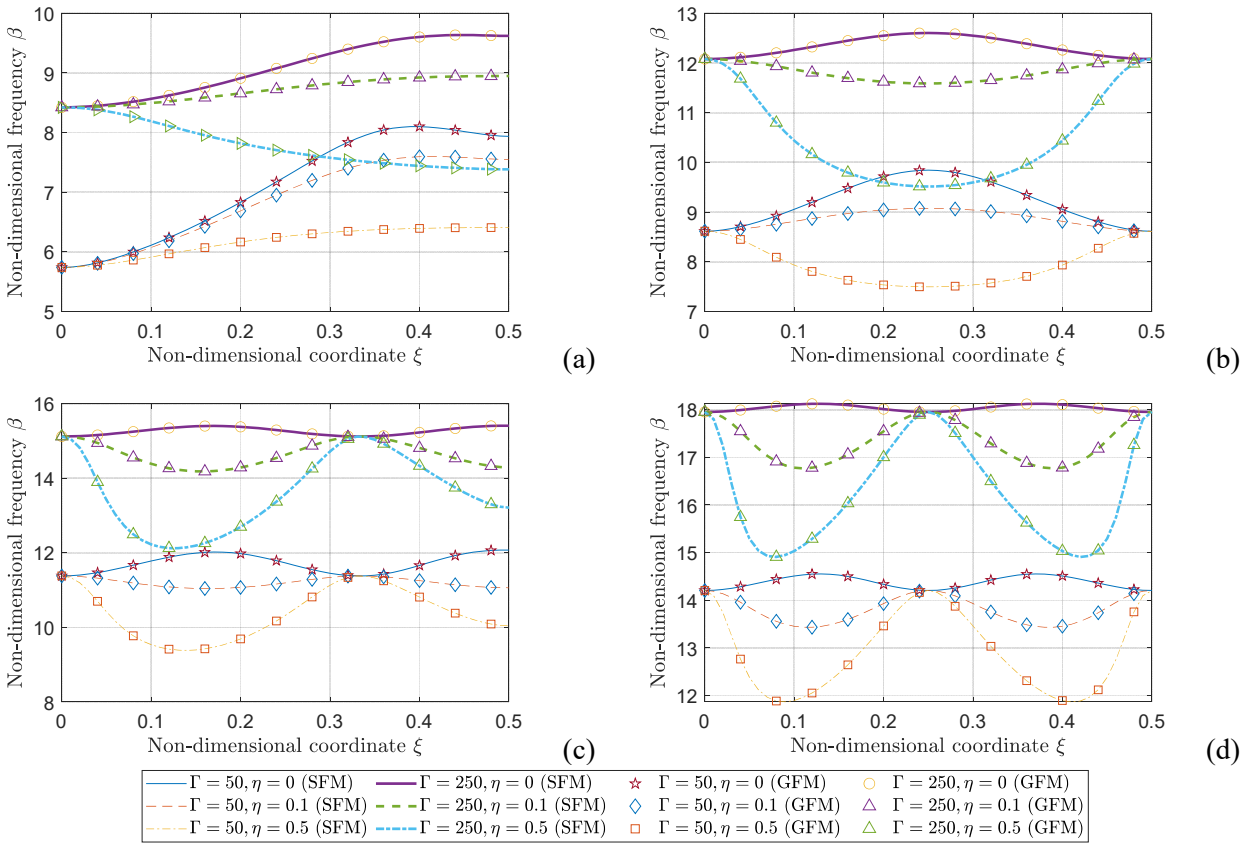

Figure 5. Comparison between the Shape Function Method (SFM) and the Green's function method (GFM) [20] for a P-P beam. (a) First mode. (b) Second mode. (c) Third mode. (d) Fourth mode

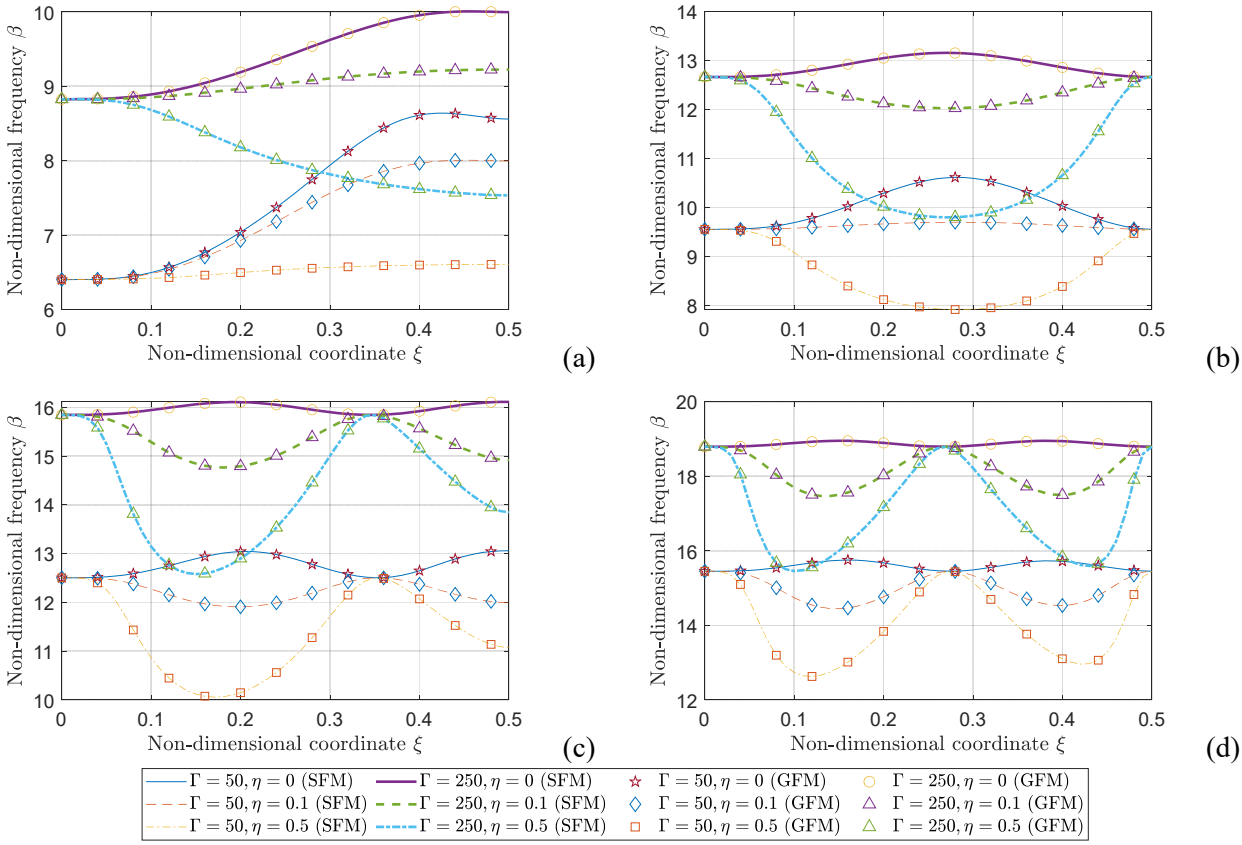

Figure 6. Comparison between the Shape Function Method (SFM) and the Green's function method (GFM) [20] for a C -C beam. (a) First mode. (b) Second mode. (c) Third mode. (d) Fourth mode

6.2. Numerical example 2

The vibration frequencies and mode shapes for a Clamped-Pinned (C-P) beam on an elastic foundation under axial force as shown in Figure 7(a) can be approached by those of a C-P beam with 100 intermediate translational elastic supports and 100 concentrated masses under the axial force in Figure 7(b), as is demonstrated in this example.

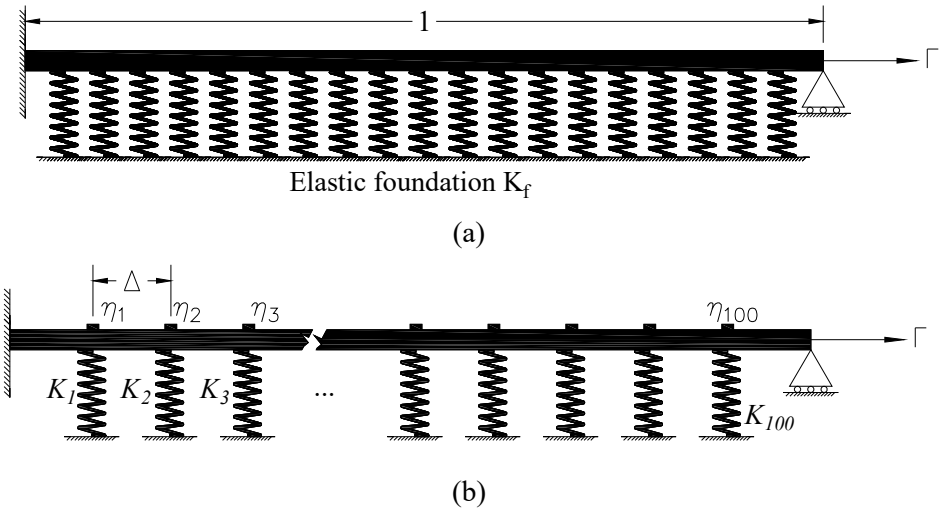

Figure 7. A C-P beam under an axial force. (a) On elastic foundation. (b) With 100 intermediate elastic supports and 100 concentrated masses

Assuming the stiffnesses of the elastic supports $K_1 = K_2 = K_3 = \cdots = K_{100}$ and the magnitude of the concentrated masses $\eta_1 = \eta_2 = \eta_3 = \cdots = \eta_{100}$ are known, then the equivalent stiffness of the elastic foundation and the additional equivalent non-dimensional mass due to the concentrated masses are obtained as

$$\boldsymbol{K_f = K_i/\Delta} \qquad (\boldsymbol{i = 1, 2, \ldots, 100}) \qquad (58)$$

$$\boldsymbol{\eta_f = \eta_i/\Delta} \qquad (\boldsymbol{i = 1, 2, \ldots, 100}) \qquad (59)$$

where K_f is the equivalent stiffness of the elastic foundation, K_i is the stiffness of each elastic support, Δ is the space between the elastic supports as shown in Figure 7(b), η_f is the additional equivalent mass of the elastic foundation, and η_i is the magnitude of each non-dimensional concentrated masses.

The governing equation of vibration of the beam on an elastic foundation shown in Figure 7(a) is formulated as,

$$\boldsymbol{\phi^{(iv)}(\xi) - 2\Gamma\phi''(\xi) - \beta_e^4\phi(\xi) = 0} \qquad (60)$$

the solution of which can be obtained by the Laplace transform method, which has a similar form as in Eqs. (43) - (47), excluding the terms involving the Dirac's delta function. After β_e is obtained, the non-dimensional vibration frequencies of the beam on elastic foundation in Figure 7(a) can be achieved by $\beta = \sqrt[4]{\frac{\beta_e^4 + K_f}{1+\eta_f}}$, and the corresponding vibration mode shapes can be graphed.

Two cases of axial force are considered in this example, i.e., $\Gamma = 50$ or 250, and the magnitude of the non-dimensional masses $\eta_i = 0.1$ $(i = 1,2,\ldots,100)$ is adopted. To consider the influences of the stiffnesses of the elastic supports, five different levels of stiffness are considered, i.e., $K_i = 1, 5, 25, 100,$ and 500. Applying Eqs. (50) and (51) the first four vibration frequencies of the beam with 100 evenly-distributed intermediate elastic supports and 100 concentrated masses under axial force (Figure 7(a)) are tabulated in

Table **2** and Table 3, together with the solutions of the beam on an elastic foundation (Figure 7(a)).

The normalized vibration mode shapes for the beam with 100 evenly-distributed intermediate elastic supports and 100 concentrated masses under axial force by the shape function method and the mode shapes of the beam on an elastic foundation are graphed in Figure 8.

It is observed in

Table **2**, Table 3, and Figure 8 that the frequency responses and mode shapes of the proposed shape function method are in excellent agreement with the solution of the vibration of an equivalent beam on an elastic foundation, suggesting that the shape function method could handle a large number of elastic supports and concentrated masses. It is worth noting that the order of the frequency equation of the beam in Figure 7(a) by the current shape function method is 2. However, for the Green's function method, the order of the frequency equation is 100, which is the same as the number of the intermediate supports or masses. The efficiency of the shape function method is justified.

Table 2. Non-dimensional frequency comparison between the SFM and the solution on an elastic foundation for a C-P beam with 100 intermediate elastic supports and 100 concentrated masses under axial force $\boldsymbol{\Gamma = 50}$

Method	Stiffness	Mode No.			
		1	2	3	4
SFM	$K_i = 1$	3.374462	4.984277	6.543467	8.124326
	$K_i = 5$	3.589767	5.056189	6.575705	8.141241
	$K_i = 25$	4.319246	5.376425	6.730183	8.224276
	$K_i = 100$	5.665775	6.241902	7.231089	8.515170
	$K_i = 500$	8.266694	8.474468	8.935084	9.712068
Elastic foundation	$K_i = 1$	3.374462	4.984277	6.543467	8.124327
	$K_i = 5$	3.589767	5.056189	6.575705	8.141242
	$K_i = 25$	4.319246	5.376425	6.730184	8.224277
	$K_i = 100$	5.665775	6.241902	7.231089	8.515171
	$K_i = 500$	8.266694	8.474468	8.935084	9.712069
Error (%)	$K_i = 1$	3.39E-07	1.84E-06	5.58E-06	1.34E-05
	$K_i = 5$	2.49E-07	1.71E-06	5.45E-06	1.32E-05
	$K_i = 25$	8.48E-08	1.26E-06	4.87E-06	1.26E-05
	$K_i = 100$	2.77E-09	5.44E-07	3.39E-06	1.06E-05
	$K_i = 500$	7.14E-08	1.49E-08	9.13E-07	5.27E-06

Table 3. Non-dimensional frequency comparison between SFM and the solution on an elastic foundation for a C-P beam with 100 intermediate elastic supports and 100 concentrated masses under axial force $\boldsymbol{\Gamma = 100}$.

Method	Foundation stiffness	Mode No.			
		1	2	3	4
SFM	$K_i = 1$	3.874091	5.616343	7.190808	8.740892
	$K_i = 5$	4.021905	5.667015	7.215156	8.754485
	$K_i = 25$	4.589408	5.901974	7.333344	8.821518
	$K_i = 100$	5.792835	6.598537	7.732213	9.060182
	$K_i = 500$	8.308677	8.625571	9.216078	10.093165
Elastic foundation	$K_i = 1$	3.874091	5.616343	7.190808	8.740893
	$K_i = 5$	4.021905	5.667015	7.215156	8.754486
	$K_i = 25$	4.589408	5.901975	7.333345	8.821520
	$K_i = 100$	5.792835	6.598537	7.732213	9.060183
	$K_i = 500$	8.308677	8.625571	9.216078	10.093165
Error (%)	$K_i = 1$	6.32E-07	2.99E-06	8.16E-06	1.80E-05
	$K_i = 5$	5.26E-07	2.86E-06	8.05E-06	1.79E-05
	$K_i = 25$	2.60E-07	2.35E-06	7.42E-06	1.72E-05
	$K_i = 100$	4.31E-08	1.30E-06	5.71E-06	1.52E-05
	$K_i = 500$	3.52E-08	1.59E-07	2.09E-06	8.58E-06

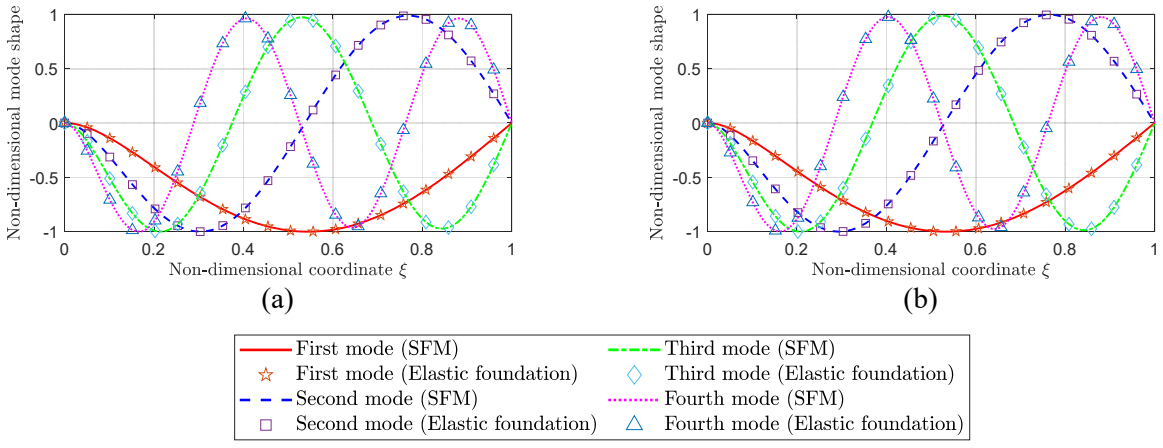

Figure 8. The first four mode shapes for a beam with 100 intermediate elastic supports and 100 concentrated masses under axial force by the shape function method and for a beam on an elastic foundation with equivalent stiffness and mass. (a) $\boldsymbol{\Gamma = 50}$. (b) $\boldsymbol{\Gamma = 100}$

7. PARAMETRIC STUDY

In this section, beams with three intermediate translational elastic supports and three concentrated masses with varied sets of boundary conditions as shown in Figure 9 are investigated. The magnitudes of the non-dimensional masses $\eta_1 = \eta_2 = \eta_4$ and the stiffnesses of the supports $K_1 = K_2 = K_3$. The relative positions of the elastic supports and the concentrated masses are $\xi_1 = 0.25, \xi_1 = 0.75,\ \xi_3 = 0.5,$ and $\xi_4 = 0.375$. It is worth pointing out that only two masses (η_1 and η_2) are colocated with two elastic supports (K_1 and K_2), while the position of the third mass η_4 is different from that of K_3 (see Figure 9). The purpose of this arrangement is to show that the position of the intermediate elastic support can be different from that of the concentrated mass, overcoming the limitations of the Green's function method developed by Kukla [20], in which the position of the supports and the masses must the same.

In this parametric study, the influences of the boundary conditions, the stiffness of the intermediate elastic supports, and the axial force on the vibration frequencies and mode shapes are investigated.

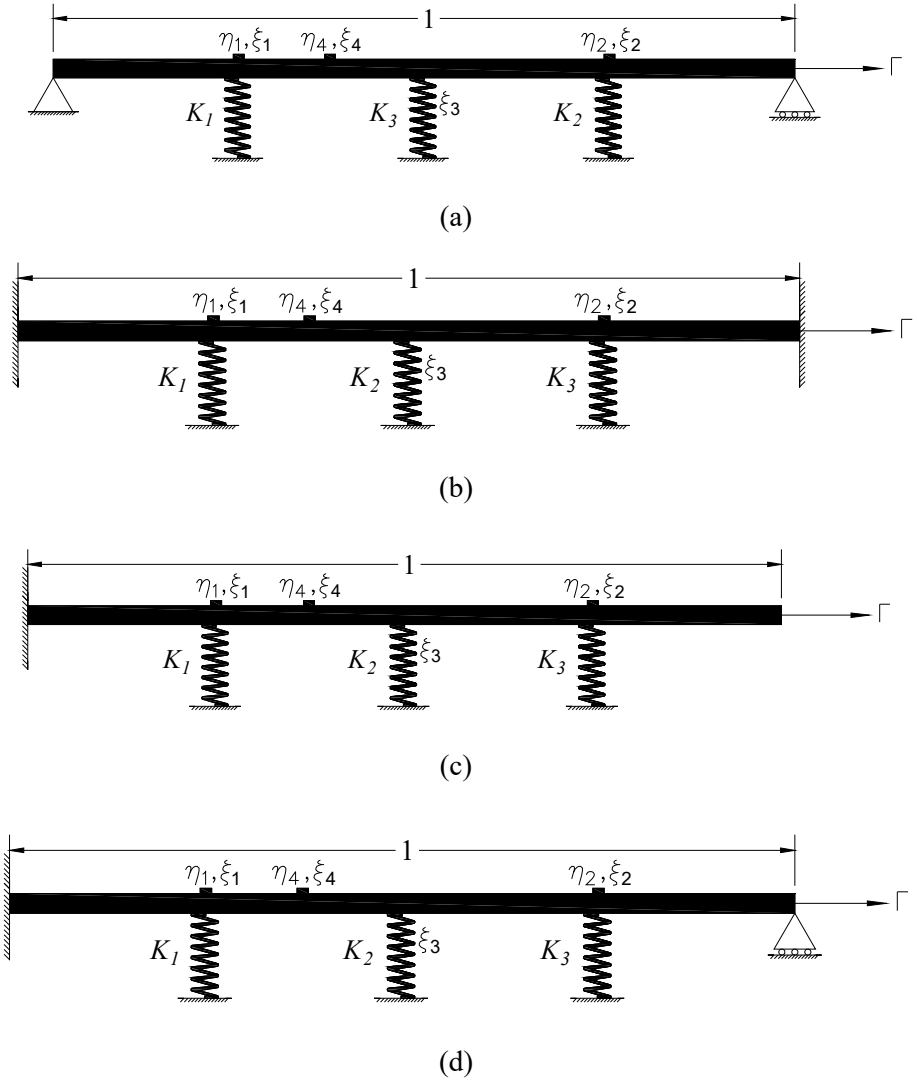

Figure 9. A beam with three intermediate elastic supports and three concentrated masses under axial force. (a) P-P. (b) C-C. (c) C-F. (d) C-P

7.1. Elastic boundary conditions

In order to show that the general solution in Eqs. (43) - (49) can accommodate many sets of boundary conditions, the conventional boundary conditions (CBC) are approached by the elastic boundary conditions (EBC) by increasing the stiffness of the translational and rotational springs as shown in Figure 10. The magnitudes of the non-dimensional masses $\eta_1 = \eta_2 = \eta_4 = 0.1$ and the stiffnesses of the supports $K_1 = K_2 = K_3 = 1000$ are applied, assuming $\Gamma = 50$.

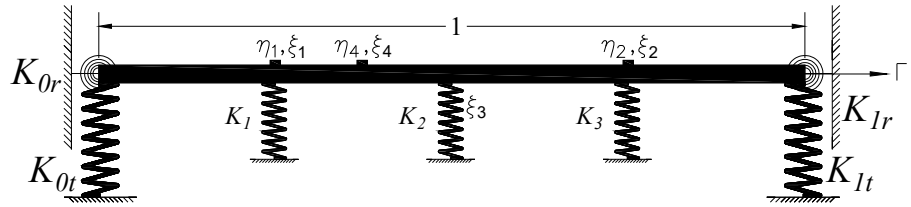

Figure 10. A beam with three intermediate elastic supports and three concentrated masses under axial force subjected to translational and rotational elastic boundary conditions

Applying Eqs. (50) - (57), the first four vibration frequencies of the beams in Figure 9 are tabulated in Table 4 and the first four mode shapes are demonstrated in Figure 11. Applying Eqs. (43) and (49), the first four vibration frequencies of the beam with three intermediate translational elastic supports and three concentrated masses are presented in Table 4 as well as the percentage errors between the CBC and EBC, and the corresponding mode shapes are graphed in Figure 11. It is observed in Table 4 that for the P-P, C-F, and C-P beam when the stiffnesses of the boundary translational and/or rotational spring are 10^6, the errors between the EBC and CBC are insignificant. However, for the C-C beam, the stiffnesses of the translational and rotational spring need to be 10^{12}, which is much higher. Besides, the first four vibration mode shapes of the beam under CBC and EBC are in good agreement. Based on the above analysis, it is remarked that the conventional boundary conditions (P-P, C-C, C-F, and C-P) can be represented by the elastic boundary conditions with sufficient translational and/or rotational stiffnesses, i.e., K_{0t}, K_{0r}, K_{1t}, and K_{1r}. In fact, the conventional boundary conditions can be simulated by setting $K_{0t} \to \infty, K_{0r} \to \infty, K_{1t} \to \infty$, and $K_{1r} \to \infty$. The interested readers may refer to Ref. [9] for more details.

Table 4. Non-dimensional frequency comparison between CBC and EBC for a beam with 3 intermediate elastic supports and 3 concentrated masses

Mode number	Label	CBC (EBC)	Non-dimensional frequency		
			CBC	EBC	Error (%)
First mode	(a)	Pinned-Pinned ($K_{0t} = K_{1t} = 10^6$, $K_{1t} = K_{1r} = 0, \Gamma = 50$)	8.027521	8.027458	7.74E-04
	(b)	Clamped-Clamped ($K_{0t} = K_{0r} = 10^{12}$, $K_{1t} = K_{1r} = 10^{12}, \Gamma = 50$)	8.324123	8.324114	9.86E-05
	(c)	Clamped-Free ($K_{0t} = K_{0r} = 10^6$, $K_{1t} = K_{1r} = 0, \Gamma = 50$)	4.319628	4.319628	2.31E-06
	(d)	Clamped-Pinned ($K_{0t} = K_{0r} = 10^6$, $K_{1t} = 10^6, K_{1r} = 0, \Gamma = 50$)	8.147256	8.147044	2.60E-03
Second mode	(a)	Pinned-Pinned ($K_{0t} = K_{1t} = 10^6$, $K_{1t} = K_{1r} = 0, \Gamma = 50$)	9.074543	9.074293	2.75E-03
	(b)	Clamped-Clamped ($K_{0t} = K_{0r} = 10^{12}$, $K_{1t} = K_{1r} = 10^{12}, \Gamma = 50$)	9.692121	9.692164	4.44E-04
	(c)	Clamped-Free ($K_{0t} = K_{0r} = 10^6$, $K_{1t} = K_{1r} = 0, \Gamma = 50$)	8.292576	8.292324	3.04E-03
	(d)	Clamped-Pinned ($K_{0t} = K_{0r} = 10^6$, $K_{1t} = 10^6, K_{1r} = 0, \Gamma = 50$)	9.390856	9.390002	9.10E-03
Third mode	(a)	Pinned-Pinned ($K_{0t} = K_{1t} = 10^6$, $K_{1t} = K_{1r} = 0, \Gamma = 50$)	11.563899	11.563107	6.85E-03
	(b)	Clamped-Clamped ($K_{0t} = K_{0r} = 10^{12}$, $K_{1t} = K_{1r} = 10^{12}, \Gamma = 50$)	12.342462	12.342052	3.32E-03
	(c)	Clamped-Free ($K_{0t} = K_{0r} = 10^6$, $K_{1t} = K_{1r} = 0, \Gamma = 50$)	9.686742	9.685987	7.80E-03
	(d)	Clamped-Pinned ($K_{0t} = K_{0r} = 10^6$, $K_{1t} = 10^6, K_{1r} = 0, \Gamma = 50$)	11.937200	11.935461	1.46E-02
Fourth mode	(a)	Pinned-Pinned ($K_{0t} = K_{1t} = 10^6$, $K_{1t} = K_{1r} = 0, \Gamma = 50$)	14.206056	14.203810	1.58E-02
	(b)	Clamped-Clamped ($K_{0t} = K_{0r} = 10^{12}$, $K_{1t} = K_{1r} = 10^{12}, \Gamma = 50$)	15.339018	15.346741	5.03E-02
	(c)	Clamped-Free ($K_{0t} = K_{0r} = 10^6$, $K_{1t} = K_{1r} = 0, \Gamma = 50$)	12.356885	12.355437	1.17E-02
	(d)	Clamped-Pinned ($K_{0t} = K_{0r} = 10^6$, $K_{1t} = 10^6, K_{1r} = 0, \Gamma = 50$)	14.723988	14.720109	2.63E-02

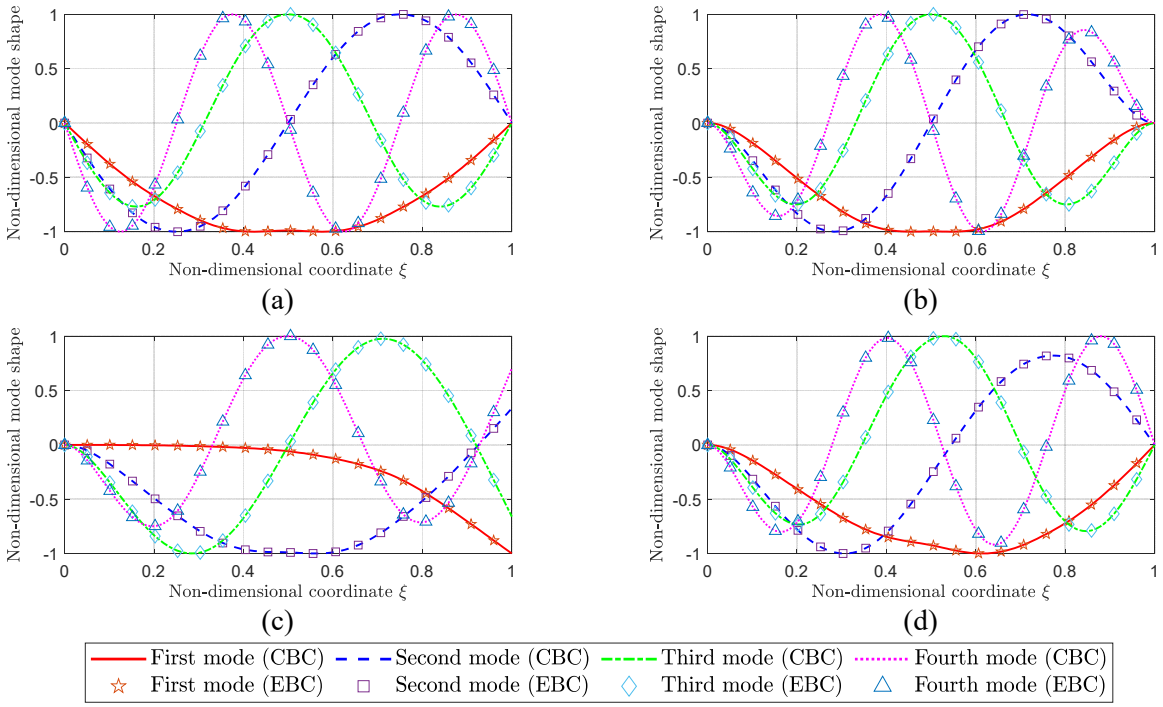

Figure 11. The first four mode shapes for a beam with 3 intermediate elastic supports and 3 concentrated masses under the CBC ((a) P-P, (b) C-C, (c) C-F, and (d) C-P) and EBC ((a) $\boldsymbol{K_{0t} = K_{1t} = 10^6, K_{1t} = K_{1r} = 0, \Gamma = 50}$, (b) $\boldsymbol{K_{0t} = K_{0r} = 10^6, K_{1t} = K_{1r} = 10^6, \Gamma = 50}$, (c) $\boldsymbol{K_{0t} = K_{0r} = 10^6, K_{1t} = K_{1r} = 0, \Gamma = 50}$, and (d) $\boldsymbol{K_{0t} = K_{0r} = 10^6, K_{1t} = 10^6, K_{1r} = 0, \Gamma = 50}$)

7.2. Influence of axial force

The influences of the axial force on the vibration frequencies and mode shapes are studied in this section. The same position parameters of the supports and masses, and the non-dimensional stiffnesses $K_i = 1000$ $(i = 1, 2, \text{and } 3)$ of the elastic supports and non-dimensional masses $\eta_i = 1000$ are adopted in this investigation. Six scenarios of the axial force are considered for the P-P beam and C-P beam, i.e., $\Gamma = 0, 50, 100, 150, 200, \text{and } 250$.

Applying the frequency equations in Eqs. (50) and (56), the calculated vibration frequencies are tabulated in

Table **5**. To better visualize the trend of the frequency change due to the increase of the axial force, the calculated frequencies in

Table **5** graphed in Figure 12. Implementing the mode shape equations in Eqs. (51) and (57), the obtained first four mode shapes of the beam with different axial forces are presented in Figure 13 and Figure 14.

Table 5. Non-dimensional frequency of a beam with three concentrated masses and three intermediate elastic supports under different boundary conditions and varied axial forces

Boundary condition	Support stiffness	Mode No.			
		1	2	3	4
P-P	$\Gamma = 0$	12.465287	12.493507	12.566371	13.000278
	$\Gamma = 50$	12.974863	12.993773	13.882409	14.206056
	$\Gamma = 100$	13.178955	13.384021	14.731551	15.418762
	$\Gamma = 150$	13.326022	13.733378	15.421708	16.398376
	$\Gamma = 200$	13.455018	14.042854	16.004181	17.228469
	$\Gamma = 250$	13.572191	14.323529	16.511628	17.953415
C-P	$\Gamma = 0$	12.471909	12.538358	12.982844	14.524617
	$\Gamma = 50$	12.984807	13.213472	14.030045	15.398398
	$\Gamma = 100$	13.226804	13.582392	14.992418	16.237103
	$\Gamma = 150$	13.387615	13.922463	15.712748	17.023595
	$\Gamma = 200$	13.521927	14.225851	16.293163	17.746045
	$\Gamma = 250$	13.641767	14.501211	16.788192	18.405007

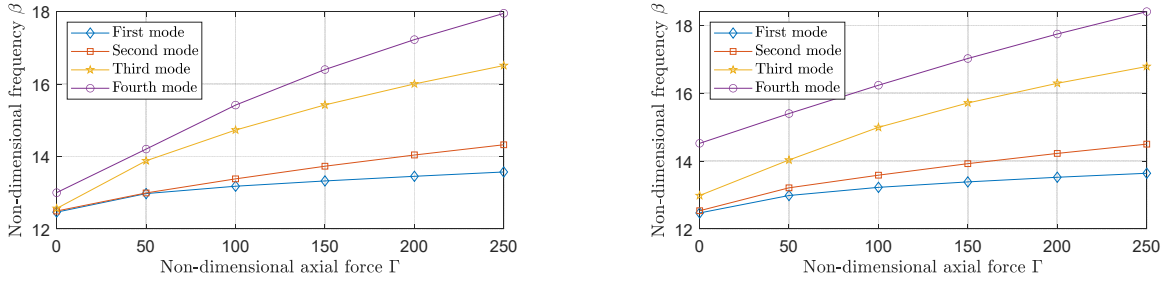

Figure 12. The first four vibration frequencies versus the axial force. (a) P-P beam. (b) C-P beam

As is shown in Figure 12 (a) and (b), the vibration frequencies increase when the axial tensile force increases for both the P-P beam and the C-P beam. However, the increasing rates of the higher modes are higher than that of the lower modes. For example, the increase rate of the second mode is higher than the first mode as is shown by the slope of the curve. For the same level of the axial force, the vibration frequencies of the first four modes of the C-P beam are higher than those of the P-P beam. This indicates that stronger restraint of the boundary conditions may result in higher vibration frequency. When the axial force is increased from 0 to 250, the vibration frequencies of the first four modes of the P-P beam are increased by approximately 8.88%, 14.65%, 31.40%, and 38.10%, respectively. The frequency increases for the C-P beam are approximately 9.38%, 15.71%, 30.28%, and 29.85%, respectively.

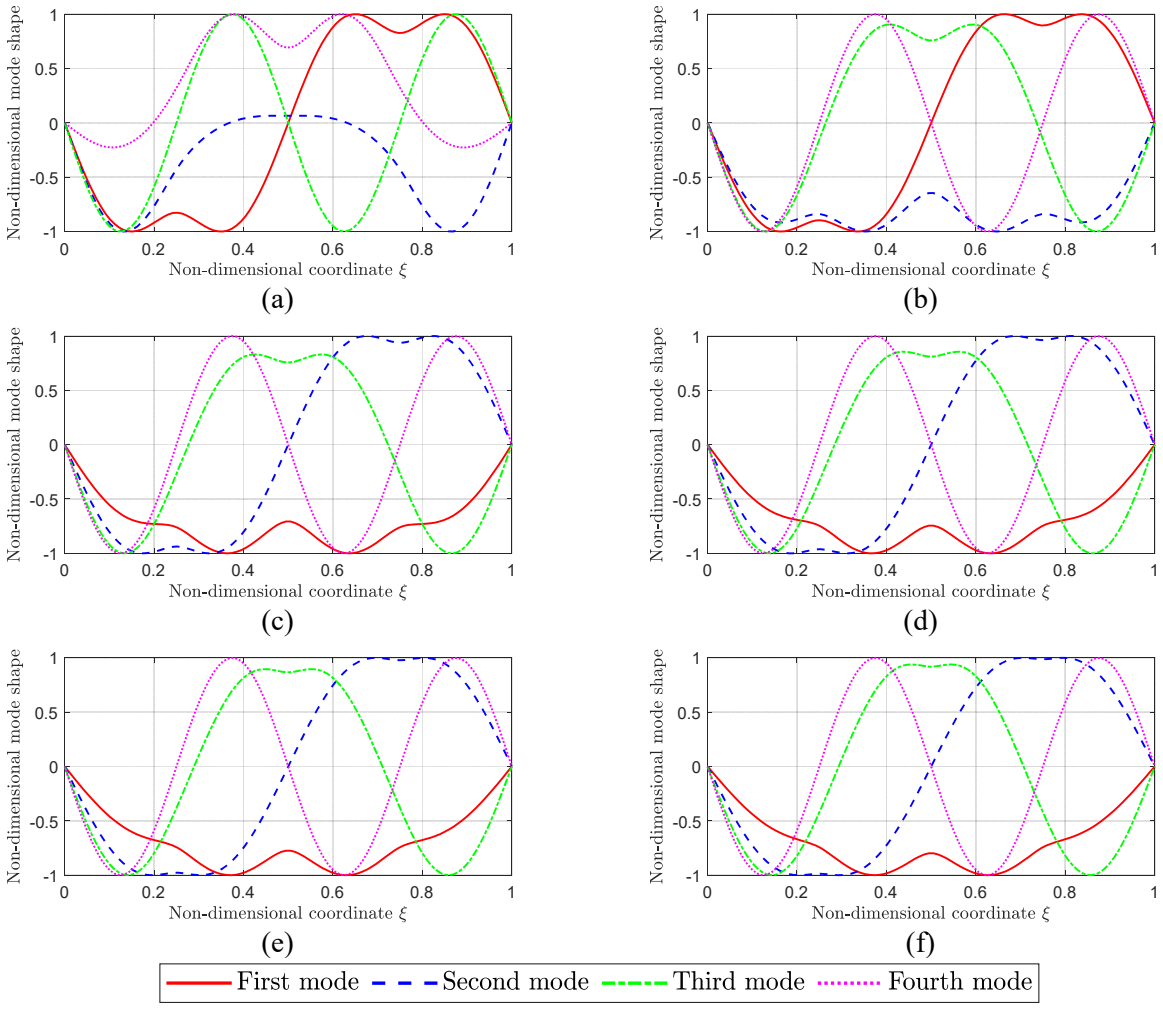

Figure 13. The first four mode shapes for a P-P beam with 3 concentrated masses and 3 intermediate elastic supports under varied axial forces. (a) $\boldsymbol{\Gamma = 0}$. (b) $\boldsymbol{\Gamma = 50}$. (c) $\boldsymbol{\Gamma = 100}$. (d) $\boldsymbol{\Gamma = 150}$. (e) $\boldsymbol{\Gamma = 200}$. (f) $\boldsymbol{\Gamma = 250}$

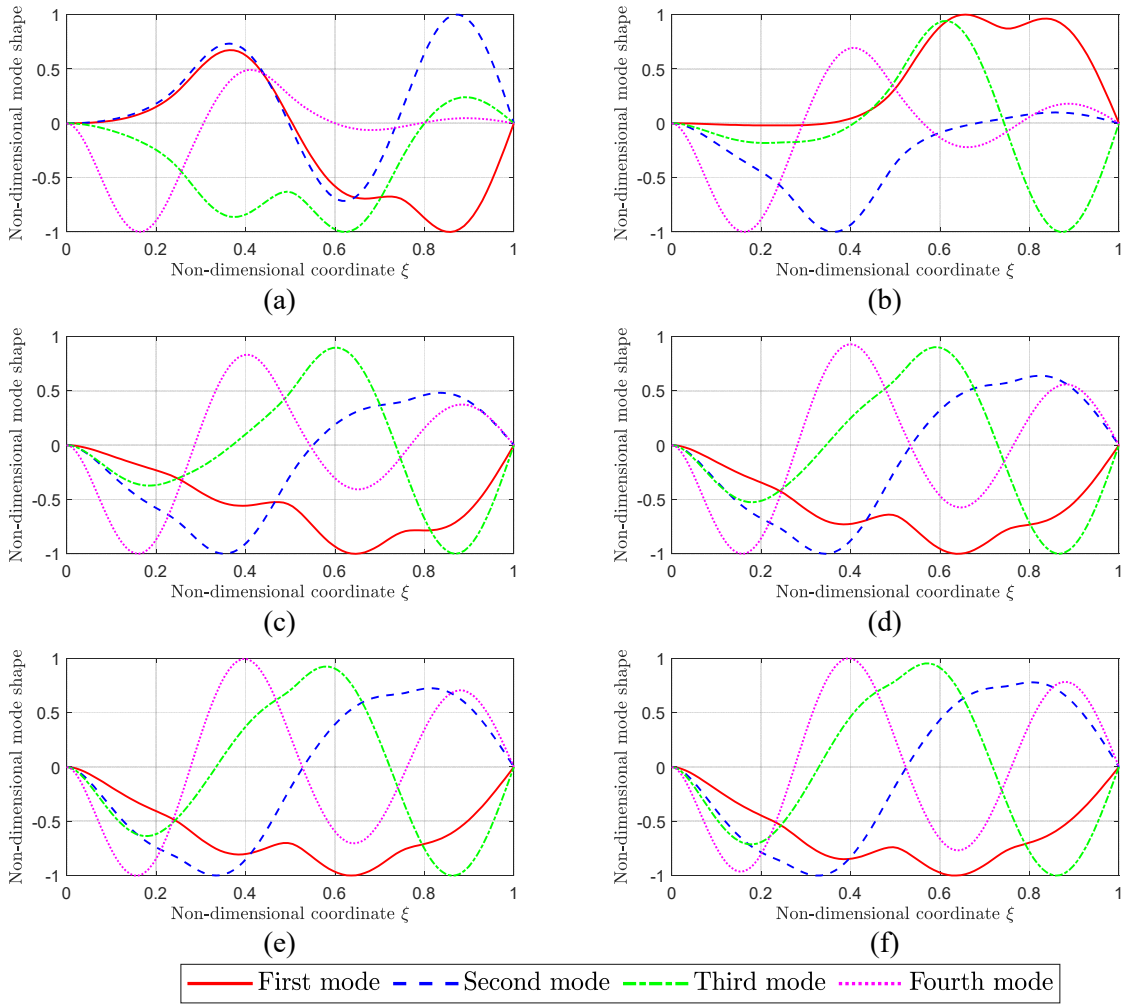

Figure 14. The first four mode shapes for a C-P beam with 3 concentrated masses and 3 intermediate elastic supports under varied axial forces. (a) $\boldsymbol{\Gamma = 0}$. (b) $\boldsymbol{\Gamma = 50}$. (c) $\boldsymbol{\Gamma = 100}$. (d) $\boldsymbol{\Gamma = 150}$. (e) $\boldsymbol{\Gamma = 200}$. (f) $\boldsymbol{\Gamma = 250}$

7.3. Influence of stiffness of elastic supports

In order to study the influences of the stiffness of the intermediate translational elastic supports, the same magnitude of masses, axial force, and position parameters as in section 7.1 are adopted. However, the stiffnesses $K_i\ (i = 1, 2, \text{and } 3)$ of the elastic supports are varied from 10 to 10^6 with a multiple of 10 for the P-P beam, C-C beam, C-F beam, and C-P beam as shown in Figure 9.

Applying the frequency equations and mode shape equations in Eqs. (50) - (57), the vibration frequencies and mode shapes are calculated. The obtained vibration frequencies are tabulated in Table 6 for varied stiffness of the supports and different sets of boundary conditions. To better visualize the trend of the frequency change due to the increase of the stiffness of the intermediate elastic supports, the calculated frequencies in Table 6 are illustrated in Figure 15. The mode shapes corresponding to varied stiffness of the elastic supports for different boundary conditions are illustrated in Figure 16 - Figure 19.

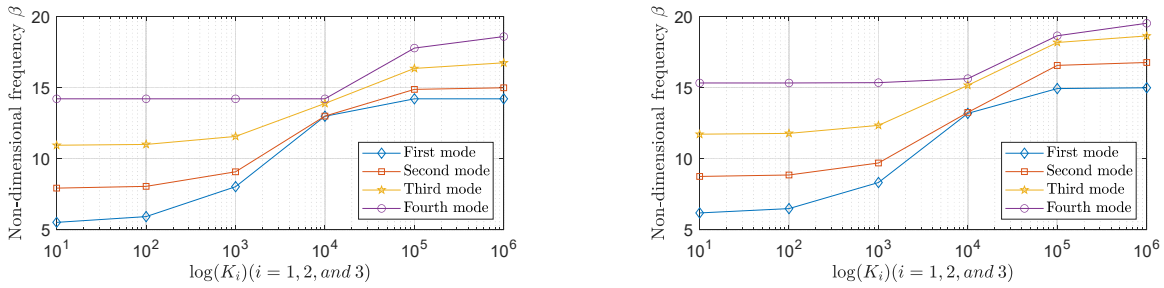

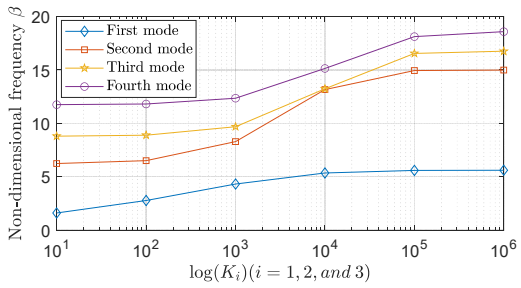

(c)

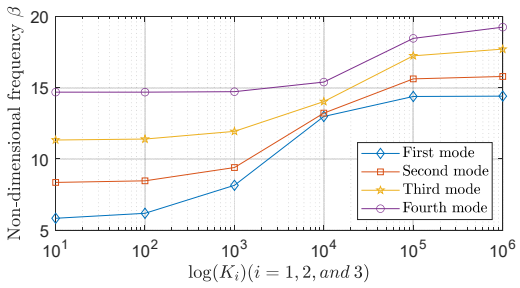

(d)

Figure 15. The first four mode shapes for a beam with 3 concentrated masses and 3 intermediate elastic supports under different boundary conditions. (a) P-P. (b) C-C. (c) C-F. (d) C-P

Table 6. Non-dimensional frequency of a beam with three concentrated masses and three intermediate elastic supports under different boundary conditions and varied stiffness

Boundary condition	Support stiffness	Mode No.			
		1	2	3	4
P-P	$K_i = 10$	5.529174	7.926972	10.942645	14.206056
	$K_i = 10^2$	5.925715	8.054925	11.005923	14.206056
	$K_i = 10^3$	8.027521	9.074543	11.563899	14.206056
	$K_i = 10^4$	12.974863	12.993773	13.882409	14.206056
	$K_i = 10^5$	14.206056	14.874086	16.340404	17.766600
	$K_i = 10^6$	14.206067	14.976411	16.734468	18.579453
C-C	$K_i = 10$	6.190090	8.746541	11.719352	15.320517
	$K_i = 10^2$	6.492628	8.847138	11.781368	15.322128
	$K_i = 10^3$	8.324123	9.692121	12.342462	15.339018
	$K_i = 10^4$	13.186767	13.250319	15.155463	15.622310
	$K_i = 10^5$	14.923560	16.550246	18.168472	18.633160
	$K_i = 10^6$	14.981614	16.754597	18.622211	19.510984
C-F	$K_i = 10$	1.603461	6.234513	8.800337	11.747663
	$K_i = 10^2$	2.777852	6.509005	8.891559	11.808000
	$K_i = 10^3$	4.319628	8.292576	9.686742	12.356885
	$K_i = 10^4$	5.346419	13.168978	13.235240	15.141204
	$K_i = 10^5$	5.584345	14.939694	16.554166	18.131201
	$K_i = 10^6$	5.612357	14.997638	16.755698	18.590831
C-P	$K_i = 10$	5.830057	8.345915	11.332046	14.690724
	$K_i = 10^2$	6.178115	8.459445	11.393225	14.693499
	$K_i = 10^3$	8.147256	9.390856	11.937200	14.723988
	$K_i = 10^4$	12.984807	13.213472	14.030045	15.398398
	$K_i = 10^5$	14.390460	15.620686	17.245443	18.474704
	$K_i = 10^6$	14.411490	15.796760	17.715547	19.259297

It is observed in Figure 15 that when the stiffness of the elastic supports increases from 10 to 10^6 with a multiple of 10, the corresponding first four vibration frequencies tend to increase. This suggests that when the stiffnesses of the translational elastic supports increases, the vibration frequencies of the beam tend to increase. The frequency variations among the four modes, except the first mode of the C-F beam in Figure 15(c), are the smallest when the stiffness of the elastic support is 10^4 for all four boundary conditions. When the stiffness of the supports is 10^6, the vibration displacements at the elastic supports are approximately zero for the P-P beam, C-C beam, C-F beam, and C-P beam, as shown in Figure 16(f), Figure 17(f), Figure 18(f), and Figure 19(f) indicating that the three elastic supports can be regarded as rigid supports. Therefore, the shape function method developed in this work could be implemented to obtain the vibration frequencies and mode shapes of a continuous beam with multi-span and an arbitrary number of concentrated masses under an axial force.

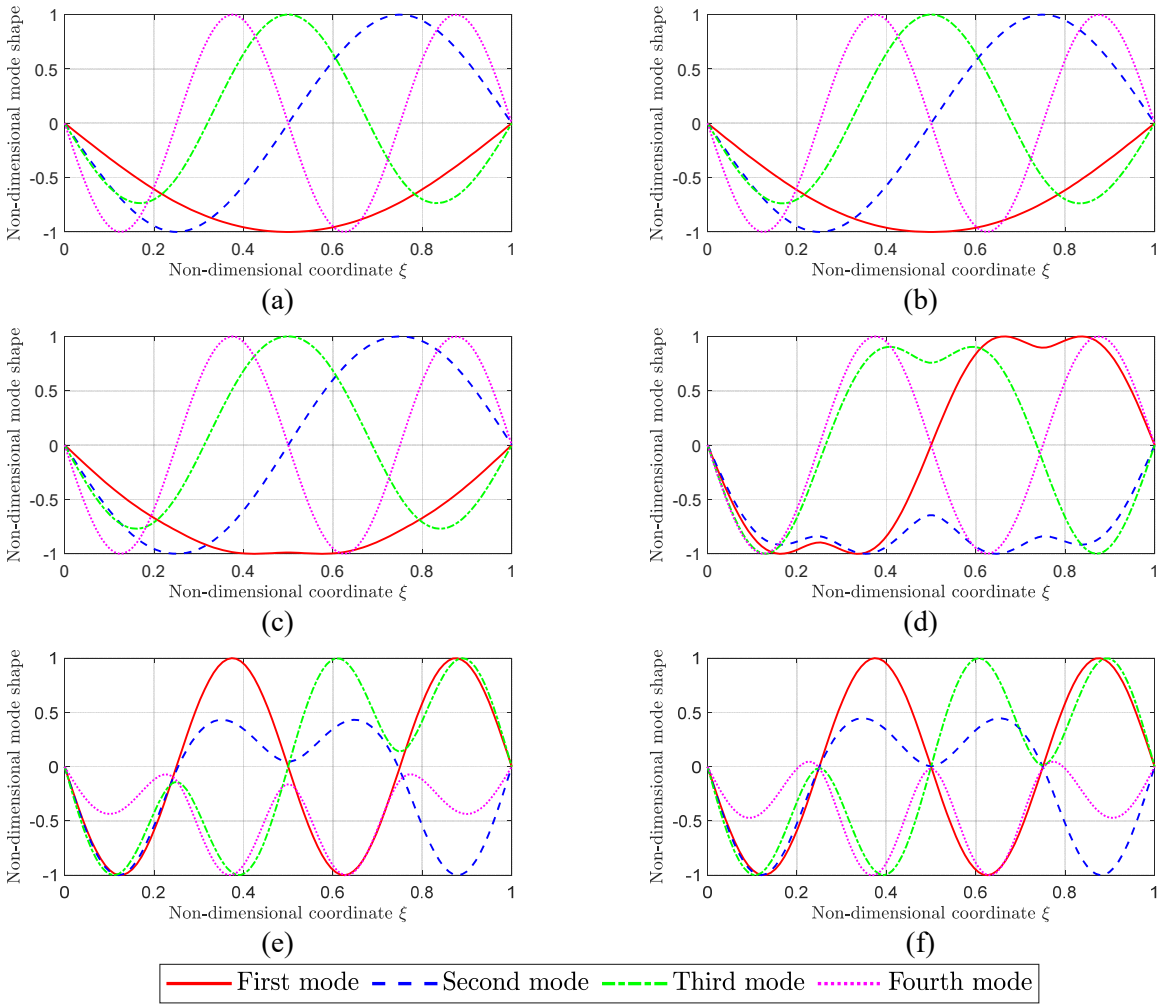

Figure 16. The first four mode shapes for a P-P beam with 3 concentrated masses and 3 intermediate elastic supports of varied stiffness. (a) $K_i = 10$. (b) $K_i = 10^2$. (c) $K_i = 10^3$. (d) $K_i = 10^4$. (e) $K_i = 10^5$. (f) $K_i = 10^6$ ($i = 1, 2,$ and 3)

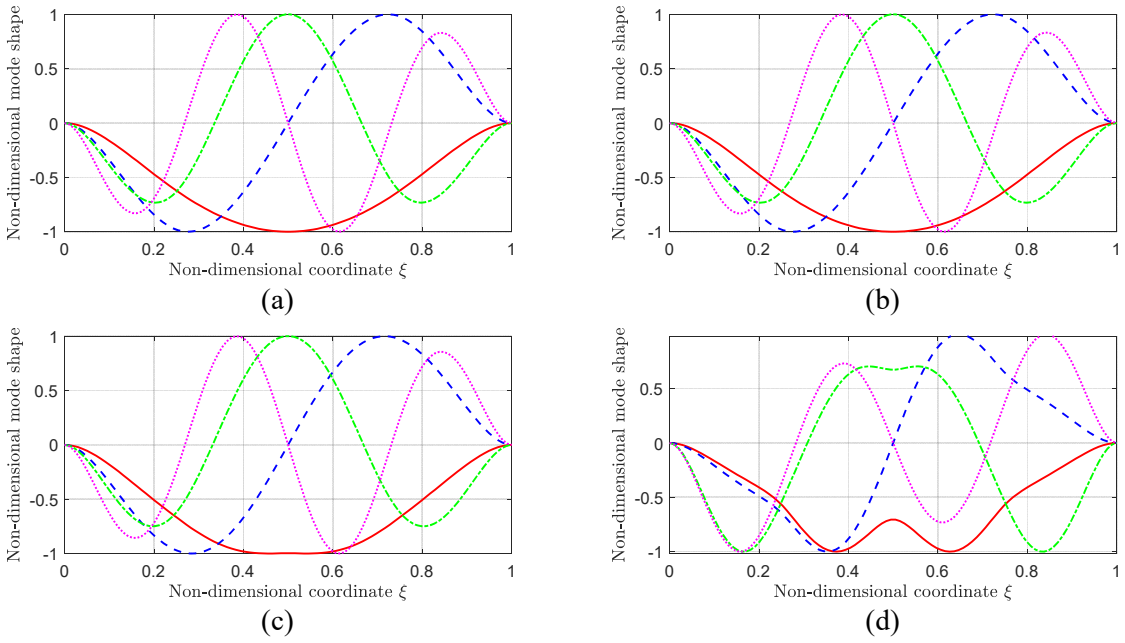

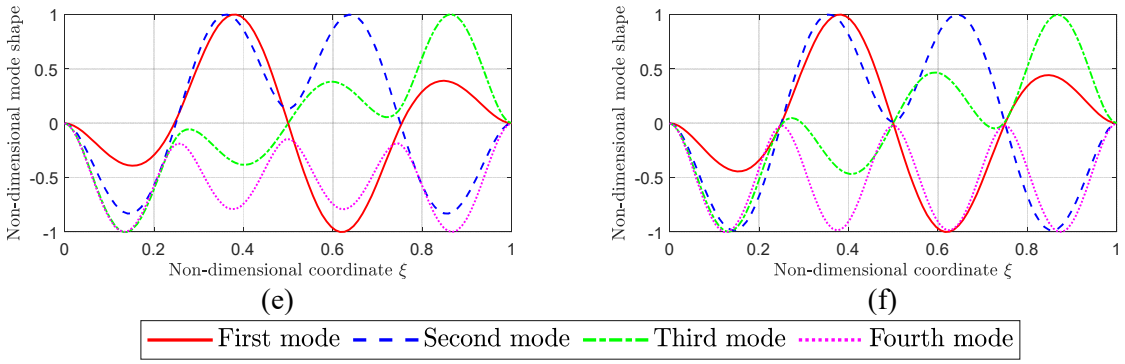

Figure 17. The first four mode shapes for a C-C beam with 3 concentrated masses and 3 intermediate elastic supports of varied stiffness. (a) $K_i = 10$. (b) $K_i = 10^2$. (c) $K_i = 10^3$. (d) $K_i = 10^4$. (e) $K_i = 10^5$. (f) $K_i = 10^6$ ($i = 1, 2,$ and 3)

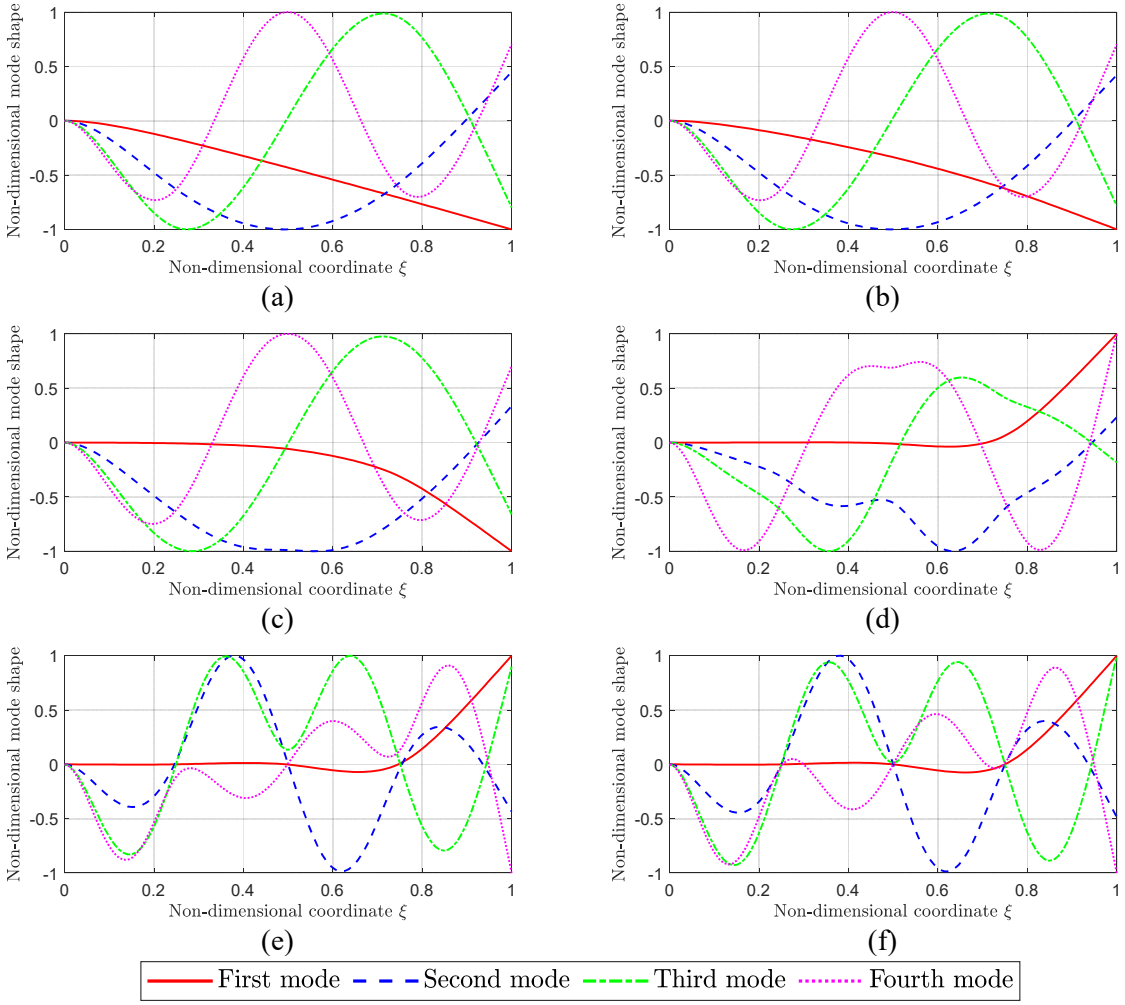

Figure 18. The first four mode shapes for a C-F beam with 3 concentrated masses and 3 intermediate elastic supports of varied stiffness. (a) $K_i = 10$. (b) $K_i = 10^2$. (c) $K_i = 10^3$. (d) $K_i = 10^4$. (e) $K_i = 10^5$. (f) $K_i = 10^6$ ($i = 1, 2,$ and 3)

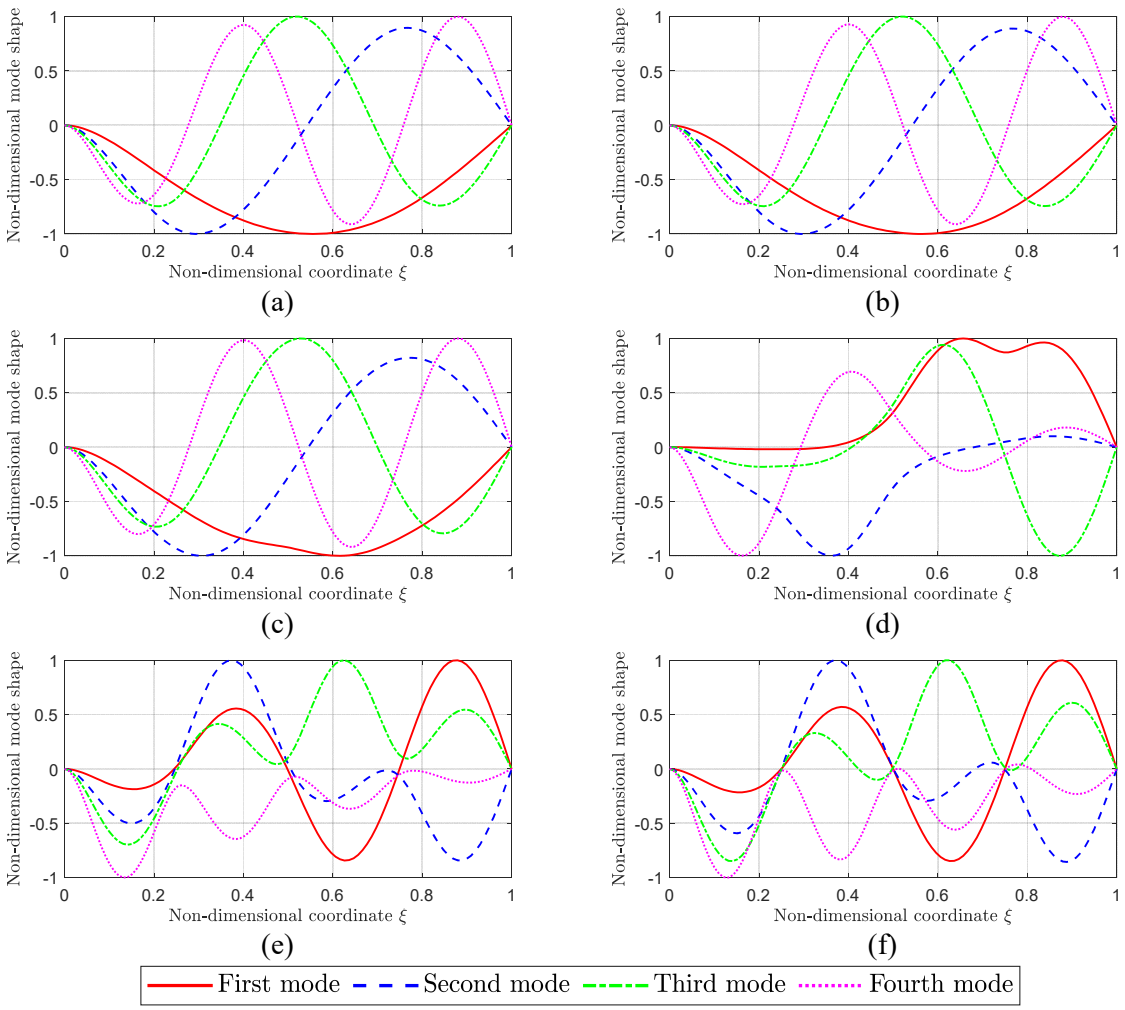

Figure 19. The first four mode shapes for a C-P beam with 3 concentrated masses and 3 intermediate elastic supports of varied stiffness. (a) $K_i = 10$. (b) $K_i = 10^2$. (c) $K_i = 10^3$. (d) $K_i = 10^4$. (e) $K_i = 10^5$. (f) $K_i = 10^6$ ($i = 1, 2,$ **and** 3)

8. CONCLUSIONS

Theoretical study of Euler-Bernoulli beams with arbitrary intermediate elastic supports and arbitrary concentrated masses under an axial force is of great interest. The exact and explicit solutions of the frequencies and mode shapes of the above-mentioned beams for the non-conventional and conventional boundary conditions are generalized by the SFM. Four new shape functions are defined. Although the concentrated masses and the axial force are included in the mathematical model, the frequency equation and mode shape function could be written in the same form as in Ref. [21], and the order of the frequency equation is still four, which does not dependent on the number of masses or the axial force.

The parametric study suggests that the conventional boundary conditions can be simulated by the non-conventional elastic boundary conditions with large boundary translational and rotational stiffnesses. Besides, the vibrations of multi-span continuous beams can be approached by increasing the stiffness of the intermediate elastic supports with the proposed method. The derived solutions are verified by the Green's function method in the literature, and vibrations of a beam under an axial force on an elastic foundation, in which good agreements are demonstrated. The proposed method in this work is potentially useful in structural health monitoring and crack detection [1-3].

Acknowledgment

The author would like to thank the two anonymous reviewers for their helpful comments and suggestions.

REFERENCES

[1] Gillich G, Ntakpe J, Wahab MA, Praisach Z, Mimis M. Damage detection in multi-span beams based on the analysis of frequency changes. Journal of Physics 2017: Conference Series2017.

[2] Praisach Z-I, Gillich N, Negru I. *Natural Frequency Changes of Euler-Bernoulli Continuous Beams with Two Spans due to Crack Occurrence*, Romanian Journal of Acoustics and Vibration, Vol.11, No.2, 2014, pp. 79-82.

[3] Ntakpe J-L, Praisach Z-I, Mituletu I-C, Gillich G-R, Muntean F. *Natural frequency changes of two-span beams due to transverse cracks*, Journal of Vibration Engineering & Technologies, Vol.5, No.3, 2017, pp. 229-238.

[4] Gillich G-R, Praisach Z-I, Abdel Wahab M, Gillich N,

Mituletu IC, Nitescu C. *Free vibration of a perfectly clamped-free beam with stepwise eccentric distributed masses*, Shock and Vibration, Vol.2016, 2016, pp.
[5] Bapat C, Bapat C. *Natural frequencies of a beam with non-classical boundary conditions and concentrated masses*, Journal of Sound and Vibration, Vol.112, No.1, 1987, pp. 177-182.
[6] Maiz S, Bambill DV, Rossit CA, Laura PAA. *Transverse vibration of Bernoulli–Euler beams carrying point masses and taking into account their rotatory inertia: Exact solution*, Journal of Sound and Vibration, Vol.303, No.3-5, 2007, pp. 895-908.
[7] Kukla S. *The Green function method in frequency analysis of a beam with intermediate elastic supports*, Journal of Sound and Vibration, Vol.149, No.1, 1991, pp. 154-159.
[8] Kukla S, Posiadala B. *Free vibrations of beams with elastically mounted masses*, Journal of Sound and Vibration, Vol.175, No.4, 1994, pp. 557-564.
[9] Rončević GŠ, Rončević B, Skoblar A, Žigulić R. *Closed form solutions for frequency equation and mode shapes of elastically supported Euler-Bernoulli beams*, Journal of Sound and Vibration, Vol.457, 2019, pp. 118-138.
[10] Štimac Rončević G, Rončević B, Skoblar A, Braut S. *A comparative evaluation of some solution methods in free vibration analysis of elastically supported beams*, Zbornik Veleučilišta u Rijeci, Vol.6, No.1, 2018, pp. 285-298.
[11] Wang L, Zhang Y, Lie ST. *Detection of damaged supports under railway track based on frequency shift*, Journal of Sound and Vibration, Vol.392, 2017, pp. 142-153.
[12] Caddemi S, Caliò I. *The influence of the axial force on the vibration of the Euler–Bernoulli beam with an arbitrary number of cracks*, Archive of Applied Mechanics, Vol.82, No.6, 2012, pp. 827-839.
[13] Laura P, de Irassar PV, Ficcadenti G. *A note on transverse vibrations of continuous beams subject to an axial force and carrying concentrated masses*, Journal Of Sound And Vibration, Vol.86, No.2, 1983, pp. 279-284.
[14] Lin S, Bapat C. *Free and forced vibration of a beam supported at many locations*, Journal Of Sound And Vibration, Vol.142, No.2, 1990, pp. 343-354.
[15] Kukla S. *Free vibration of a beam supported on a stepped elastic foundation*, Journal of Sound and Vibration, Vol.149, No.2, 1991, pp. 259-265.
[16] Kukla S. *Application of Green functions in frequency analysis of Timoshenko beams with oscillators*, Journal of Sound and Vibration, Vol.205, No.3, 1997, pp. 355-363.
[17] Mohamad A. *Tables of Green's functions for the theory of beam vibrations with general intermediate appendages*, International Journal of Solids and Structures, Vol.31, No.2, 1994, pp. 257-268.
[18] Abu-Hilal M. *Forced vibration of Euler–Bernoulli beams by means of dynamic Green functions*, Journal of Sound and Vibration, Vol.267, No.2, 2003, pp. 191-207.
[19] Sun L. *A closed-form solution of a Bernoulli-Euler beam on a viscoelastic foundation under harmonic line loads*, Journal of Sound and Vibration, Vol.242, No.4, 2001, pp. 619-627.
[20] Kukla S. *Free vibrations of axially loaded beams with concentrated masses and intermediate elastic supports*, Journal of Sound and Vibration, Vol.172, No.4, 1994, pp. 449-458.
[21] Chang P, Zhao X. *Exact solution of vibrations of beams with arbitrary translational supports using shape function method*, Asian Journal of Civil Engineering, Vol.21, No.7, 2020, pp. 1269-1286.
[22] Ahlborn T, Shuchman R, Sutter L, Brooks C, Harris D, Burns J, et al., *The state-of-the-practice of modern structural health monitoring for bridges: a comprehensive review*, 2010, pp.
[23] Barke D, Chiu WK. *Structural health monitoring in the railway industry: a review*, Structural Health Monitoring, Vol.4, No.1, 2005, pp. 81-93.
[24] Farrar CR, Worden K. *An introduction to structural health monitoring*, Philosophical Transactions of the Royal Society A: Mathematical, Physical and Engineering Sciences, Vol.365, No.1851, 2006, pp. 303-315.
[25] Friswell MI, Penny JE. *Crack modeling for structural health monitoring*, Structural Health Monitoring, Vol.1, No.2, 2002, pp. 139-148.
[26] Rabelo DdS, Hobeck JD, Inman DJ, Neto RMF, Jr. Steffen V. *Real-time structural health monitoring of fatigue crack on aluminum beam using an impedance-based portable device*: Sage Publications Ltd; 2017.
[27] Sepehry N, Bakhtiari-Nejad F, Shamshirsaz M, Zhu W. *Nonlinear modeling of cracked beams for impedance based structural health monitoring*: Amer Soc Mechanical Engineers; 2018.
[28] Sohn H, Farrar CR, Hemez FM, Czarnecki JJ. A review of structural health review of structural health monitoring literature 1996-2001. Los Alamos National Laboratory; 2002.
[29] Sohn H, Farrar CR, Hemez FM, Shunk DD, Stinemates DW, Nadler BR, et al., *A review of structural health monitoring literature: 1996–2001*, Los Alamos National Laboratory, USA, 2003, pp.
[30] Ghannadiasl A, Ajirlou SK. *Forced vibration of multi-span cracked Euler-Bernoulli beams using dynamic Green function formulation*: Elsevier Sci Ltd; 2019.
[31] Zhao X, Hu QJ, Crossley W, Du CC, Li YH. *Analytical solutions for the coupled thermoelastic vibrations of the cracked Euler-Bernoulli beams by means of Green's functions*: Pergamon-Elsevier Science Ltd; 2017.
[32] Zhao X, Zhao Y, Gao X, Li X, Li Y. *Green′ s functions for the forced vibrations of cracked Euler–Bernoulli beams*, Mechanical Systems and Signal Processing, Vol.68, 2016, pp. 155-175.
[33] Zhao X, Zhao YR, Gao XZ, Li XY, Li YH. *Green's functions for the forced vibrations of cracked Euler-Bernoulli beams*: Acad. Press Elsevier Science Ltd; 2016.
[34] Zhao X. *Automated rotational- and scaling-invariant image-based crack width monitoring with sub-millimeter accuracy and self-numbering label*, Asian Journal of Civil Engineering, Vol.21, No.4, 2020, pp. 741-749.
[35] Zhao X. *Free Vibration Analysis of Cracked Euler-Bernoulli Beam by Laplace Transformation Considering Stiffness Reduction*, Romanian Journal Of Acoustics And Vibration, Vol.16, No.2, 2020, pp. 166-173.
[36] Fu C. *The effect of switching cracks on the vibration of a continuous beam bridge subjected to moving vehicles*: Academic Press Ltd- Elsevier Science Ltd; 2015.
[37] Nguyen KV. *Comparison studies of open and breathing crack detections of a beam-like bridge subjected to a moving vehicle*, Engineering Structures, Vol.51, 2013, pp. 306-314.
[38] Tan G, Wang W, Jiao Y. *Free vibration analysis of a cracked simply supported bridge considering bridge-vehicle interaction*: Journal Vibroengineering; 2016.
[39] Zhou L, Liu H. *Response of cracked simply supported concrete beam with moving vehicle load*: Ernst & Sohn; 2016.
[40] Zhao X. *Analytical solution of deflection of multi-cracked beams on elastic foundations under arbitrary boundary conditions using a diffused stiffness reduction crack model*, Archive of Applied Mechanics, 2020, doi: 10.1007/s00419-00020-01769-00411 (In press).
[41] Rao SS. *Vibration of continuous systems*: John Wiley & Sons Ltd; 2019.
[42] Caddemi S, Caliò I, Cannizzaro F. *Tensile and compressive buckling of columns with shear deformation singularities*, Meccanica, Vol.50, No.3, 2015, pp. 707-720.